Microporous and Mesoporous Materials 336 (2022) 111874

Contents lists available at ScienceDirect

Microporous and Mesoporous Materials

journal homepage: www.elsevier.com/locate/micromeso

Sol-gel derived silica: A review of polymer-tailored properties for energy and environmental applications

Karthikeyan Baskaran [a,1], Muhammad Ali [a,1], Katherine Gingrich [b], Debora Lyn Porter [b], Saehwa Chong [c], Brian J. Riley [c], Charles W. Peak [d], Steven E. Naleway [b], Ilya Zharov [b], Krista Carlson [a,*]

[a] University of Nevada Reno, Reno, NV, 89557, USA
[b] University of Utah, Salt Lake City, UT, 84112, USA
[c] Pacific Northwest National Laboratory, Richland, WA, 99354, USA
[d] Texas A&M University, College Station, TX, 77843, USA

ARTICLE INFO

Keywords:
Polymer
Silica
Aerogel
Xerogel
Composite
Hybrid

ABSTRACT

With the continuous growth in global population, energy demands are summoning the development of novel materials with high specific surface areas (SSA) for energy and environmental applications. High-SSA silica-based materials, such as aerogels, are highly popular as they are easy to form and tune. They also provide thermal stability and easy functionalization, which leads to their application in batteries, heavy metal adsorption, and gas capture. However, owing to large pore volumes, high-SSA silica exhibits weak mechanical behavior, requiring enhancement or modification to improve the mechanical properties and make them viable for these applications. The creation of macropores in these mesoporous solids is also desirable for applications utilizing membranes. To facilitate research in these critical areas, this review describes the research into sol-gel formation of silica, as well as polymer-based tailoring carried out in the last decade. Additionally, this review summarizes applications of polymer-tailored high-SSA silica materials in the energy and environmental fields and discusses the challenges associated with implementing and scaling of these materials for these applications.

1. Introduction

New technologies are needed to meet the expanding energy demands of the rapidly increasing global population. The need to improve the performance of energy conversion and storage (ECS) systems to meet these demands is driving the development of new materials. Simultaneously, unique materials are also being explored to mitigate the environmental impacts of these technologies. In both cases, sol-gel derived silica-based materials, such as aerogels and xerogels, have been receiving increasing attention due to their unique intrinsic properties: high (greater than hundreds of $m^2\ g^{-1}$) SSAs, ease of formation and functionalization, tunable pore structures, chemical inertness, and thermal stability [1,2]. While high-SSA silica has proven to be functionally effective, it suffers from low mechanical strength and ductility, which limits its ability to be broadly implemented [3,4]. The poor mechanical profile of high-SSA silica is related to its large pore volume that results in concentration of stresses on its limited load-sustaining solid network [5]. Additionally, intrinsic pore structure tunability facilitated by modifications during the silica sol-gel process is limited because of its stochastic nature, which can be improved by using external porogens [6–11].

Over the years, researchers have explored various methods to improve mechanical properties and tune the pore structures of high-SSA silica in a fashion where the intrinsic properties are preserved [12,13]. The use of polymers to make composites or hybrids have proven to be some of the most effective strategies to improve mechanical behavior of high-SSA silica [14–17]. Polymers have also been successfully used as porogens to enable finely tuned pore structures [7–11]. Table 1 includes some examples of high-SSA silica modified using polymers and the improvements in properties [15,18–31].

The enhancement of properties and control over pore structure has enabled high-SSA useful for many energy and environmental applications. For example, in ECS systems, high-SSA silicas are typically used to

* Corresponding author.
E-mail address: kc@unr.edu (K. Carlson).
[1] equal contribution.

https://doi.org/10.1016/j.micromeso.2022.111874
Received 15 December 2021; Received in revised form 11 March 2022; Accepted 28 March 2022
Available online 5 April 2022

Abbreviations

APTES	(3-aminopropyltriethoxysilane)
APTES	(3-aminopropyltriethoxysilane)
BPGE	(bisphenol A propoxylate diglycidyl ether)
BTESB	(1,4-bis(triethoxysilyl)-benzene)
BTESE	(bis(triethoxysilyl)-ethane)
BTMSH	(1,6-bis(trimethoxy-silyl)hexane)
BTMSPA	(bis(trimethoxysilylpropyl)amine)
CMCD	(carboxymethylated curdlan)
CNF	(cellulose nanofibrils)
CNF	(cellulose nanofibrils)
DI	(di-isocyanate)
FMW	(formulated molecular weight)
ICPTES	(3-isocyanatopropyl triethoxysilane)
MTMS	(methyltrimethoxysilane)
PEDS	(polyethoxydisiloxane)
PEG	(polyethylene glycol)
PEO	(polyethylene oxide)
PMMA	(poly(methyl methacrylate))
PS	(Polystyrene)
PVA	(polyvinyl alcohol)
SA	(sodium alginate)
SI-ATRP	(surface initiated atom transfer radical polymerization)
TDI	(toluene diisocyanate)
TEOS	(tetraethyl orthosilicate)
THEOS	(tetrakis-(2-hydroxyethyl) orthosilicate)
TMCS	(trimethylchlorosilane)
TMMA	(tri methyl methacrylate)
TMOS	(tetramethyl orthosilicate)
TMSPM	(3-(trimethoxysilyl)propyl methacrylate)
TMS-PNP	([trimethoxysilyl-modified poly(butyl metacrylate) shell and a poly(butyl metacrylate-co-butyl acrylate) core] - polymer nanoparticle)
VTMS	(vinyltrimethoxysilane)

Table 1
Enhanced properties of silica-polymer composites or hybrids. Note that SA and SX stand for silica aerogel and silica xerogel, respectively, and the polymer abbreviations are defined in the text.

Gel	Polymer	Enhanced properties	Ref(s)
SA, SX	PDMS	Flexibility and rubber-like elasticity, improved fracture toughness, hydrophobicity, optical clarity, mechanical stability	[18–23]
SA	PAN	Enhanced chemical durability and thermal stability	[24]
SX	PAN	Higher Pb^{2+} capturing efficiency and larger specific surface area compared to silica xerogel,	[25]
SA	PVP	Enhanced compressive strength, optical transparency, hydrophobicity.	[26]
SA	PMMA-TMSPM		
SA	PDMS		
SA	PDMA		
SA	PMMA	Improved thermal properties compared to PMMA	[15]
SX	PMMA	Transparent to visible light, mechanical properties like PMMA, improved hydrophobicity	[27]
SA	PS	Improved hydrophobicity, rubbery	[28]
SA	PEG	Improved mechanical strengths and thermal insulation	[29,30]
SA, SX	PEO	High mechanical durability against compression	[31]

provide a thermally and chemically stable support for the active species, such as catalysts in fuel cells, thermally stable substrates for photocatalysts in H_2 and O_2 production by water splitting, or porous structure to facilitate higher ionic conductivity [32–34]. The addition of polymers provide salt-solvating, mechanical strength and electrochemical stability [35–37]. For environmental applications involving remediation, high-SSA silica provide more sites for adsorption of pollutants and polymers provide properties such as mechanical strength and sorption specificities [38]. The use of polymers as porogens enables a high level of pore structure tunability to create interconnected and/or hierarchical pore structures that enable better adsorption [7–11].

Reviews on high-SSA silica in the last 10 years have focused on general sol-gel processing without polymers, polymer-silica composites, inorganic-organic hybrids, or their applications [2,39–44]. This review will fill in gaps in summarizing the most recent advances in the use of polymers to tailor the mechanical properties and pore structure of high-SSA silica, specifically for energy and environmental applications (Fig. 1). Within these applications, this review will focus on the energy storage applications of materials designed for batteries, and the environmental applications on materials used to capture environmental pollutants. This review concludes with a discussion on the challenges associated with scaling laboratory methods and the implementation of these materials in their desired applications.

2. Sol-gel synthesis

Sol-gel synthesis methods are often used to produce high-SSA silica due to the ease with which chemical and physical properties can be controlled through compositional adjustments [60,61]. For silica, sol-gel processing is commonly performed using the precursor tetraethoxysilane (TEOS, also called tetraethyl orthosilicate), which carries ethoxide groups ($–OC_2H_5$) [62]. When TEOS, which is typically dissolved in an organic solvent, is mixed with an aqueous solution of a catalyst, hydrolysis and condensation reactions will occur to form the silica network of the gel. General hydrolysis and condensation reactions are shown in Eqs. (1)–(4), where R represents an alkyl [60,61]. Either acidic or basic catalysts (in varying concentrations) can be added to accelerate the rates of these reactions.

Hydrolysis:

$$(Partial)\quad Si(OR)_4 + H_2O \rightarrow (OR)_3SiOH + ROH \qquad \text{Eq. 1}$$

$$(Complete)\quad Si(OR)_4 + 4H_2O \rightarrow Si(OH)_4 + 4ROH \qquad \text{Eq. 2}$$

Condensation:

$$(OR)_3SiOR + HOSi(OR)_3 \rightarrow (OR)_3SiOSi(OR)_3 + ROH \qquad \text{Eq. 3}$$

$$(OR)_3SiOH + HOSi(OR)_3 \rightarrow (OR)_3SiOSi(OR)_3 + H_2O \qquad \text{Eq. 4}$$

Organosilanes that carry both alkoxy (i.e., R–O) and silyl (e.g., $Si–CH_3$) groups are often used as precursors or co-precursors to introduce non-polar groups to create high-SSA silica with enhanced ductility and hydrophobicity [63]. Fig. 2 shows some common oxysilanes and organosilianes used as precursors and functionalizing components and resulting end groups on the silica network.

Upon formation of a gel and following a solvent exchange process, drying can be performed using supercritical fluids (critical point drying) to produce aerogels, freeze drying to produce cryogels, or ambient pressure (e.g., aerogels or xerogels) [32,64]. Each method has benefits and challenges in regard to ease of use, property control, and scalability. Due to the highly microporous and mesoporous nature of high-SSA silica, aerogels or xerogels tend to have poor mechanical properties (i.e., brittle, low strength) regardless of the processing method, limiting

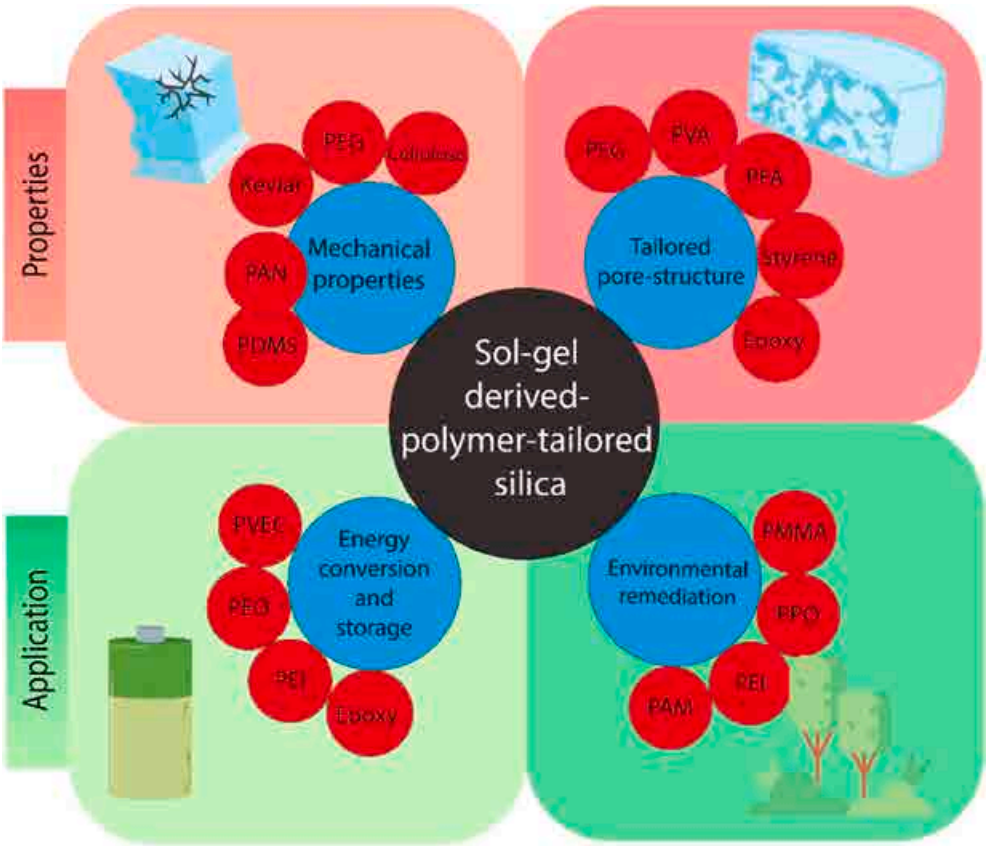

Fig. 1. Overview of polymers used for tailoring silica properties. The two quadrants at the top represent the polymers used in enhancing properties of the high-SSA silica [8,9,23,45–52] and the lower two quadrants represent the polymers whose properties combined with high SSA values show enhanced performance [53–59].

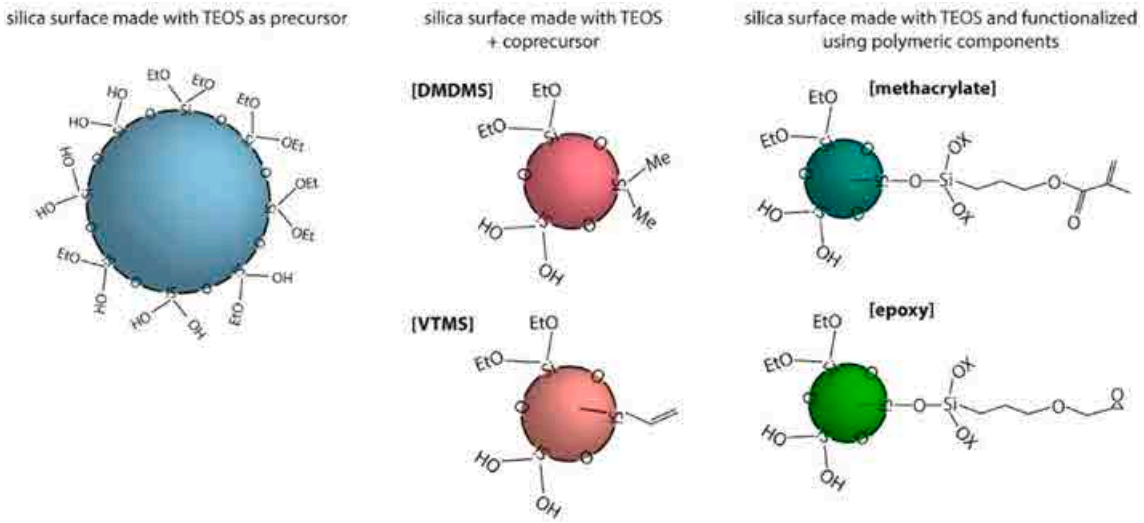

Fig. 2. Common oxysilanes and organosilianes used as precursors and functionalizing components, and the resulting end groups on the silica network. DMDMS refers to dimethyl dimethoxysilane and VTMS refers to vinyltrimethoxysilane.

prospective use in realistic and industrial settings [3,65].

To alleviate this problem, polymers can be incorporated into these structures to form composites or hybrid materials to enhance mechanical properties, such as strength, failure stress, and compressive modulus. Additionally, polymers can be used as sacrificial templates (i.e., porogens) to tailor the microstructure and obtain interconnected macropores and/or hierarchical pore structures [6,66]. Precursors can be coupled with specific polymers based on chemical compatibilities, which depend on the silyl groups of the precursors (Fig. 3).

3. Polymers for enhanced mechanical properties

Polymers can be used to enhance the strength, ductility, and toughness of native high-SSA silica by creating composites or hybrids [43,67–72]. Polymer incorporation in silica sol-gels can also mitigate shrinkage and cracking issues during ambient-pressure drying.

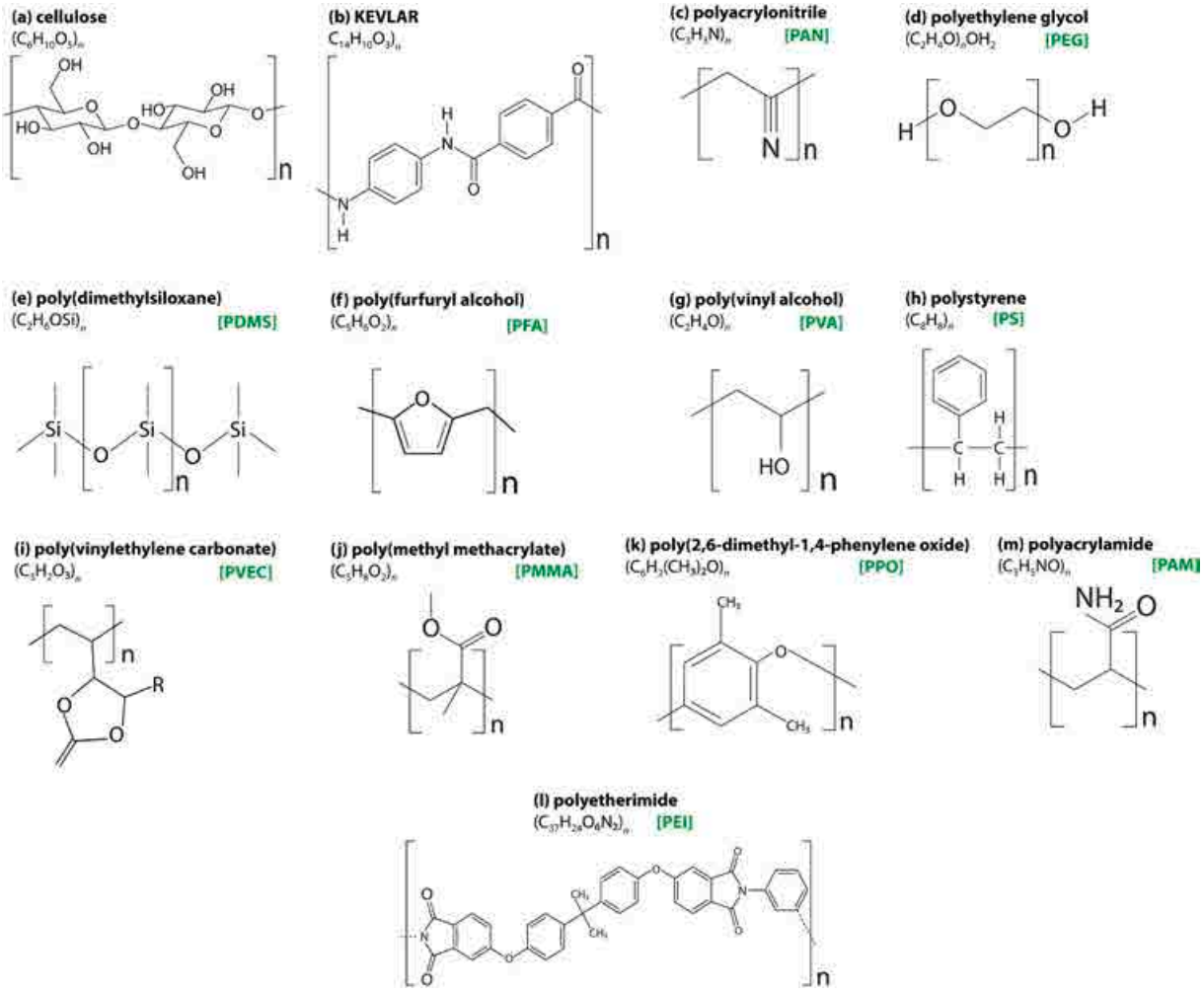

Fig. 3. Structure of common polymers used to tailor the properties of high-SSA silica.

Composites are multiphase materials that are formed when materials with dissimilar chemical or physical properties undergo macrolevel mixing, such that the individual properties of the components are combined and enhanced [73–75]. Compounds in hybrids mix on a molecular level for the creation of a new material exhibiting properties that may not be present in the individual components (Fig. 4) [76–79]. The use of co-precursors with silyl end groups is aimed to assist in the formation of both composites and hybrids through surface cross-linking with appropriate polymers [80–82].

3.1. Polymer-reinforced silica composites

Polymer-reinforced silica composites are comprised of two separate entities, which are the matrix and the filler. Polymer-silica composites

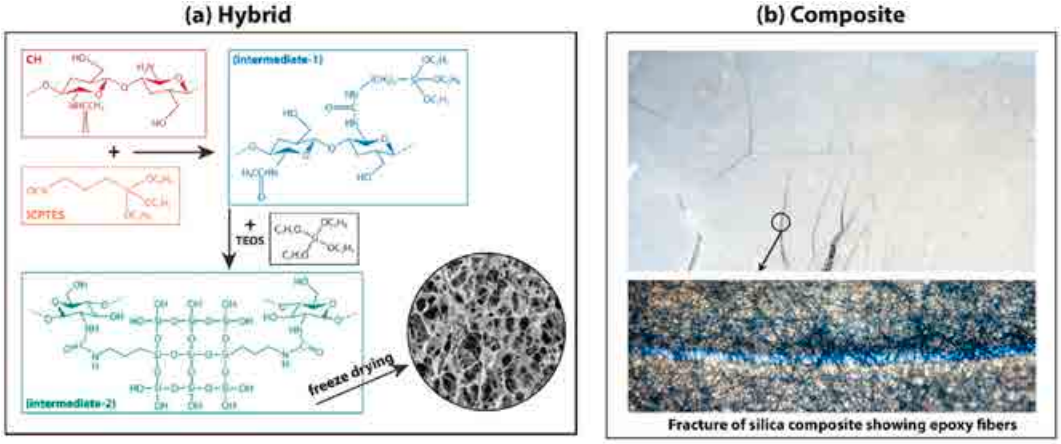

Fig. 4. Fundamental comparison between (a) shows molecular interactions with no distinct phases between chitosan and ICPTES to create a hybrid material and (b) shows macrolevel interaction with distinct phases corresponding to silica and a polymer-fiber [23,83].

are categorized into two groups based on their interfacial chemistry: (1) physically embedded polymer filler in the silica matrix bonding via van der Waals or electrostatic forces and (2) composites developed through covalent bonds between the polymer filler and silica matrix [13,84]. In the first case, the overall strength and toughness of the material is improved due to polymer agglomeration, which inhibits crack propagation through the solid. In the second case, the stronger interface between the chemically bonded filler and matrix typically leads to a composite with a higher strength than those with only electrostatic or van der Waals forces [85]. In both cases, effective dispersion of the filler material and good interfacial compatibility are critical to ensure an even stress distribution across the material, thus resulting in high mechanical properties of the composite [70,86].

Polyacrylonitrile (PAN) [47] and cellulose [87] are among the common cost-effective polymers that lead to the formation of mechanically strong composites. Specialty polymeric fibers such as Kevlar [46] and TENCEL [48] have been used to develop composites with tailored mechanical properties. The mechanical properties of some notable polymer-reinforced silica composites are summarized in Table 2 [23,45,46,87–94].

PAN is a versatile polymer with impressive mechanical characteristics that can be combined with silica through electrospinning to make composites [95,96]. For example, PAN fibers with a length of 50 mm and a diameter of 10 (±2) μm were used to develop PAN-silica composites that showed an increased compression modulus, from 180 kPa in native silica aerogels to 260 kPa with addition of 0.3 w/w% PAN fibers [47].

Cellulose, a biodegradable and biocompatible polymer, has also been used to create aerogel scaffolds with enhanced mechanical properties [45,88,89,92]. As a natural and abundant material, cellulose offers a sustainable method to tailor the properties of aerogels, thus reducing their environmental impact. The inclusion of cellulose nanofibrils consistently increased the compression modulus with various precursors: sodium silicate (Na_2SiO_3) from 43 kPa to 75 kPa [89], TEOS from 180 kPa to 5420 kPa [92], and TEOS-methyltrimethoxysilane (MTMS) from 2.5 kPa to 69.1 kPa [45]. In another study, the addition of silica to aerogels formed from bacterial cellulose was shown to enhance the mechanical strength [87]. The addition of a sodium silicate precursor to the mesh-like cellulose network produced by the bacteria increased the compression modulus from 0.27 MPa to 16.67 MPa with 96.9 w/w% silica.

3.2. Polymer-modified silica hybrids

Hybrid materials are a combination of two components that integrate at the molecular level to create materials with new properties [97–100]. Pertinent to high-SSA silica, organically modified silica called an ormosil incorporate organics with oxides derived from sol-gel processes. By varying polymers in the structures, unique properties can be achieved including rubbery (high ductility) behavior, enhanced hardness and mechanical strength, hydrophobicity, and corrosion resistance [18,19,101,102]. Ormosils are generally synthesized by three different methods described below [101,102]. In the first method, the organic precursor is mixed with the gel precursor solution and is trapped during gelation without chemically bonding to the oxide network. In the second

Table 2
The mechanical properties of high-SSA polymer-reinforced silica. Cells with '–' represent that specific data was not provided in the listed literature. Moduli, stresses, and strains were determined using compression tests, unless otherwise noted (*) which were determined using flexural testing. Catalysts used are reported outside the parenthesis and co-precursor, if used, is reported in the parentheses.

Silica Precursor	Catalyst (Co-precursor)	Polymer Components	Interaction	Composition	Avg. Modulus (MPa)	Avg. Ultimate or Maximum Stress (MPa)	Avg. Strain at failure or Maximum Strain (%)	Ref
MTMS	HCl	CNF	Covalent	0.5 CNF (wt%)	0.0025	-	-	[45]
				1.0 CNF (wt%)	0.0093	-	-	
				2.0 CNF (wt%)	0.0691	-	-	
PEDS	NH_4OH	TENCEL® Cellulose Fibers	-	0 TENCEL® (vol%)	2.59*	0.0463*	1.9*	[88]
				1.13 TENCEL® (vol %), 2 mm fibers	3.40*	0.0608*	3.1*	
				1.14 TENCEL® (vol %), 6 mm fibers	5.15*	0.1362*	4.2*	
				1.12 TENCEL® (vol %), 8 mm fibers	5.00*	0.1227*	4.0*	
				1.10 TENCEL® (vol %), 12 mm fibers	5.88*	0.2866*	5.3*	
Sodium Silica	HCl (APTES)	CNF	Hydrogen Bonding	4:6 CNF:Silica (vol ratio)	0.043	0.0175	80	[89]
				6:4 CNF:Silica (vol ratio)	0.075	0.0178	80	
	H_2SO_4	Bacterial Cellulose Fibers	Hydrogen Bonding	36.4 SiO_2 (wt%)	0.38			[87]
				69.5 SiO_2 (wt%)	0.52			
				93.7 SiO_2 (wt%)	3.70			
				96.9 SiO_2 (wt%)	16.67			
TEOS	HCl, NH_3	TMS-PNP	Covalent Bond	0 TMS-PNP nanoparticle (wt%)	28	0.92	5.1	[91, 94]
				3 TMS-PNP nanoparticle (wt%)	44	4.24	14.4	
	HCl, NH_4OH (TMCS)	Aramid (Kevlar®) Fibers	Electrostatic	2.7 Kevlar® (vol%)	0.512*	0.06*		[46]
				4.1 Kevlar® (vol%)	0.912*	0.088*		
				5.4 Kevlar® (vol%)	1.24*	0.115*		
				6.6 Kevlar® (vol%)	1.42*	1.38*		
	HCl, NH_4OH	PEO	Van der Waal	1.9 PU fiber (wt%)	5-10*	0.15–0.20*	8-10*	[23]
	HCl, NH_4OH	CNF	Covalent	0 SiO_2 (wt%), pH of 10	5.93	1.44		[92]
				51.9 SiO_2 (wt%), pH of 10	5.42	1.38		
				100 SiO_2 (wt%), pH of 10	0.18–0.47	0.047–0.16		
	HCl, NH_3 (MTMS)	Bacterial Cellulose Fibers	-	83.9 SiO_2 wt%	0.485	0.280	60	[93]

method, the organic precursor is mixed with the gel precursor solution and chemically bonded to the oxide network comprising the gel. In the third method, the organic precursor is impregnated into a premade and porous oxide-gel structure. Several notable ormosils are shown in Fig. 5, and possible structures of a polydimethylsiloxane (PDMS)-based ormosil are shown in Fig. 6 [15,48,103–109]. Table 3 summarizes the mechanical properties of some notable polymer-modified silica hybrids [16,17,68,83,110–118].

PDMS is a common, chemically stable and water-resistant polymer used to synthesize ormosils [18,19,21]. Varying the amount of added PDMS enables changes in the elasticity, mechanical strength, and optical transparency in the final ormosil product. In a typical ormosil synthesis process, a higher PDMS content increases the porosity and ductility of ormosils, but decreases the tensile strength [19]. Ormosils synthesized using silica xerogel and PDMS with a TEOS/PDMS mass ratio of <1.5 results in a rubber-like elasticity [19]. Organically modified silica aerogels (aeromosils) have also been synthesized using PDMS [18]. Higher PDMS contents resulted in higher ductility but a reduced SSA values [18]. Electrospun nanofiber membranes incorporated with PDMS silica aerogels have been demonstrated for membrane distillation [21]. The effects of the aerogel concentrations in the precursor solution in the range of 10–70% have been found to have significant effects on the membrane functionality. Membrane properties including superhydrophobicity, surface energy and roughness, and liquid entry pressure were largely dependent on the organic polymer concentration during gelation.

PAN is another common, chemically stable and water-resistant polymer used to synthesize ormosils. For example, it can be dissolved in dimethyl sulfoxide, mixed with silica gel particles and then dried to obtain a high-SSA fused silica membrane [119]. After treatment with a TEOS solution, the material undergoes a sol-gel transition to form a silica network around the fused silica particles [119]. It was shown that having this dense network of fused silica particles improved gas selectivity by permeation for an O_2/N_2 mixture.

TEOS-PMMA hybrids were developed using methacrylate-copolymers via the reversible addition-fragmentation chain transfer (RAFT) polymerization technique [17]. The synthesis included the preparation of these copolymers with three different structures: linear (3D), random, and star. All three variants showed significant ductility before reaching their failure points during a uniaxial compression test. They also exhibited a high ultimate compressive stress, a high failure strain, a low compressive modulus, and a high energy required to failure.

Natural polymers such as chitosan and alginate have also been used to modify the mechanical properties of silica. Chitosan-silica hybrids were developed using a sol-gel process that included a variety of chitosan and SiO_2 compositions and the addition of either acetic acid or HCl to vary the pH [111]. It was observed that weak acidic condition during the sol-gel reaction favored the development of better mechanical strength and toughness. A hybrid with 50 wt% chitosan exhibited the highest compressive strength of 42.6 $\pm$ 3.3 MPa when tested under wet conditions using deionized water and 271 $\pm$ 31 MPa when tested dry. In a similar study, improved mechanical strength (up to 95 MPa) and stability was observed in chitosan-silica hybrids [83]. A TMOS-alginate hybrid was developed for biomedical applications with improved mechanical properties [114]. All experimented variants of this hybrid with different mixture compositions showed an increased compressive modulus, compressive strength, and work of fracture when compared to the native materials. The highest values for compression modulus (1270 kPa) and compressive strength (1200 kPa) were observed in samples with 20 wt% alginate and 80 wt% silica.

Silica aerogels modified with polymers derived from precursors such as toluene diisocyanate (TDI), di-isocyanate (DI) and tris[2-(acryloyloxy)ethyl] isocyanurate have been explored to develop hybrids that exhibit improved mechanical properties. Amine-modified silica was used with varying TDI concentrations to produce hybrid gels that were dried under ambient pressure without producing significant cracks [112]. Results showed a decrease in elastic moduli (from 1.20 MPa at 0% TDI to 0.26 MPa at 20% TDI) and compressive strength (from 1.20 MPa at 0% TDI to 0.26 MPa at 20% TDI) of the hybrid with the addition of polymers but showed a significant improvement in sustaining higher strain (from 6.35% at 0% TDI to 45.93% at 20% TDI).

Similarly, the effects of tri-methacrylate derived from tris[2-(acryloyloxy)ethyl] isocyanurate crosslinking on silica was investigated [117]. Reinforcement with tri-methacrylate improved the mechanical properties of the aerogels as the maximum strength (400 kPa) observed was significantly higher than the non-reinforced aerogels (10 kPa). Crosslinking of silica with polyurea derived from DI produced hybrids with improved mechanical strength, with the highest polymer concentration yielding a maximum stress of 340 MPa [115].

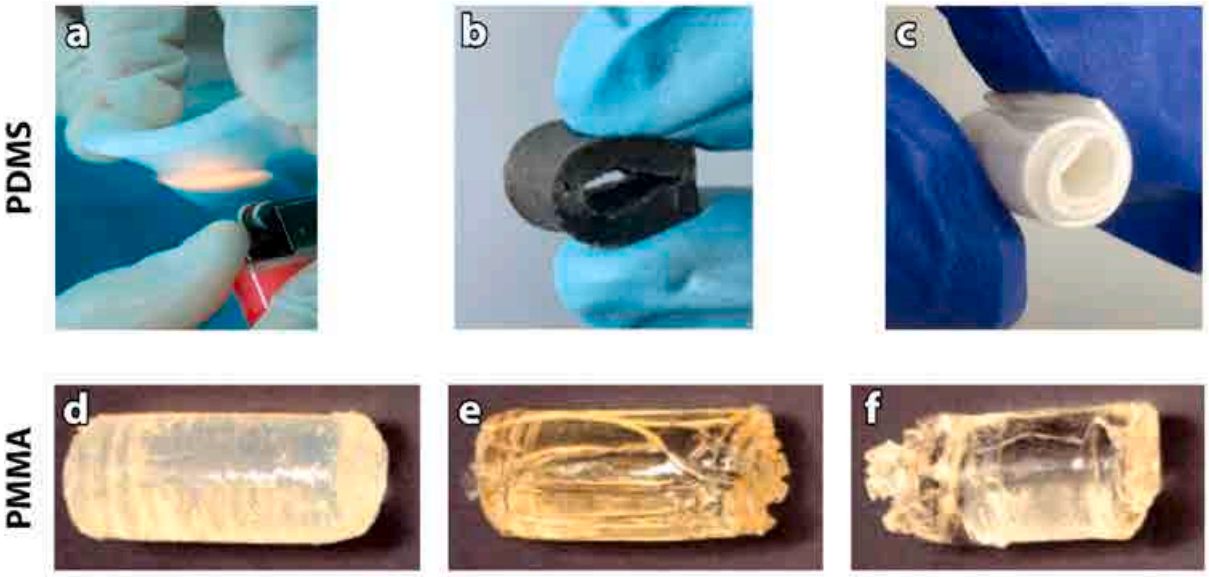

Fig. 5. Optical images of polymer-composite gels from the literature including those constructed with (a–c) PDMS (a [48], b [104] c [105]) and (d–e) PMMA ([15]). These figures were modified from the originals and reprinted with permission.

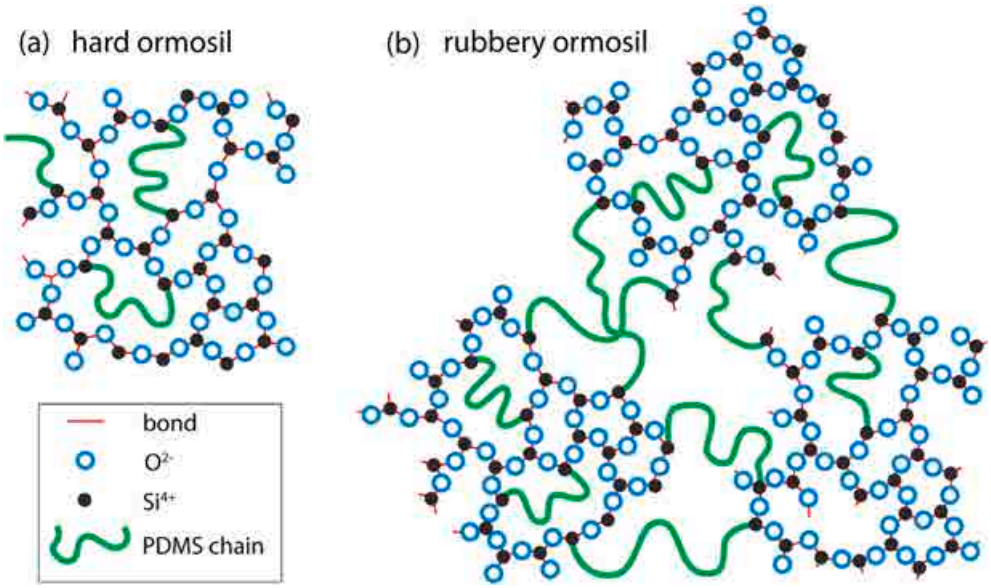

Fig. 6. Proposed structures of SiO_2-PDMS hybrids for (a) hard ormosils (low PDMS content) and (b) rubbery ormosils (high PDPMS content). This figure is based on reference [102] and was reprinted with permission.

4. Polymers for tailoring pore structure

Micropores and mesopores are responsible for the high-SSA in sol-gel derived silica. The intrinsic pore structure formed during sol-gel synthesis can be altered and enhanced using porogens, which are removable materials that use physical and/or chemical interactions with the silica for the deliberate design of non-intrinsic pore structures (e.g., macropores, long-range interconnected pores) [120]. Fine tuning of the pore structure can be achieved by adjusting the concentration of polymer or the physical parameters of the sol (e.g., stirring speed, temperature). Based on the literature, we have broadly classified the porogens as either hard templates or soluble polymers based on the type of interaction they have with the sol-gel solution. Hard templates were classified as polymers whose phase does not change during the sol-gel reaction. For soluble polymers, miscibility with the sol-gel solution may change over time as the condensation reactions proceed. In either case, porogens are removed after the gel formation or drying, leaving tailored pore structures (Fig. 7).

4.1. Hard templates

Polystyrene (PS) [9,50], polymethyl methacrylate (PMMA) [51], and poly(e-caprolactone) (PCL) [10] are a few examples of polymers classified as hard templates. Interactions between the polymer and silica during the sol-gel reaction are limited to surface reactions and have little effect on the properties or form of the polymer used in template. Before being added to the sol, the surfaces of the polymer particles are often modified with functional groups that favor interactions with silica oligomers to assist in the uniform dispersion of the polymeric porogen within the sol-gel solution. Since the polymer does not dissolve during the sol-to-gel transition, the resulting pore volume of the macropores and pore morphology are governed by the size, shape, and concentration of the porogen(s) [9,11,66].

High-SSA silica gels with hierarchical pore structures have been created using PCL [11] templates treated with 3-aminopropyltrimethoxylsilane (APTMS) and PS [9] templates treated with 3-isocyanatopropyltriethoxysilane (Fig. 7(b)). In the case of PCL, gels were first vacuum dried and then subjected to pyrolysis for porogen removal. The resulting average size of the micropores in silica gels after the removal of polymer was observed within the range of 2–10 μm which mimics the size of the template itself (i.e., 5–10 μm). In addition to the micropores, nanopores in the size of ~2 nm were observed that were due to the presence of grafting polymer chains on the polymer microspheres [11].

An advantage of using hard templates is that they do not require precise control over the sol-gel reaction parameters to obtain a hierarchical pore structure. However, as templates are designed to be insoluble in the solvents used during sol-gel processing, post-synthesis heat treatments (~550 °C) are required to remove the porogen [9,11]. These treatments can be unfavorable as pyrolysis of the porogen can leave a carbon-based residue that can alter the final properties in an undesired way [64,66]. Additionally, the higher temperatures required for polymer decomposition can lead to sintering of the microstructure and removal the organic functional groups present on the surface of the silica gel, limiting the prospects of further functionalization or surface modification [8].

4.2. Soluble polymers

When control over pore structure is required at length scales ranging from nanometers to micrometers, soluble polymers that can mix with the precursor at the molecular level are desirable. Common soluble polymers include PEG [122,123], poly (furfuryl alcohol) (PFA) [52], and PVA [8]. As the sol-gel reaction proceeds, the miscibility of the polymer and precursor-containing solvent tends to change. The resulting phase separation can be controlled to tailor the pore structure by controlling the rate of polymerization of the silica oligomers and the type of polymeric interactions with the silica network as it evolves. Depending on the level of interaction between the polymer and the silica during the gel formation, distinct silica-solvent and solvent-polymer phases (nucleation and growth) form or silica-polymer-rich and silica-solvent-rich phases (spinodal decomposition) form as shown in Fig. 7(c) [124–128]. When using soluble polymers as porogens, both the molecular weight of the polymer and the solvent are critical in providing control over the microstructure [122,123].

The influences of the solvent, the precursor, and porogen are shown in Fig. 8. In the event of phase separation, the volume fraction of the micropores is governed by the solvent and the polymer, whereas the volume fraction of macropores is governed only by the polymer. In either system, the influence of the porogen does not necessarily cease after the gel formation. It can continue during aging, a process in which the gel network is left to coarsen in the mother liquor or a solvent exchange medium. The aging process with suitable solvent will also

Table 3
Polymer modified silica aerogel mechanical properties. Modification is provided by both natural and synthetic polymers. Empty cells represent that specific data was not provided in the listed literature. Moduli, stresses, and strains were determined using compression tests, unless noted (*) which were determined using flexural testing. Catalyst is reported outside the parenthesis and co-precursor, if used, is reported in the parentheses.

Silica Precursor	Catalyst (Co-precursor)	Polymer Components	Composition	Avg. Modulus (MPa)	Avg. Ultimate or Maximum Stress (MPa)	Avg. Strain at failure or Maximum Strain (%)	Ref.
MTMS	HCl	PVA, CNF	1:1 PVA:CNF (weight ratio)	0.1207	0.056	80	[110]
TEOS	CH_3COOH, HCl	Chitosan (tested wet)	50 Chitosan, 50 Silica (wt%)	314	42.6	41.7	[111]
			60 Chitosan, 40 Silica (wt%)	132	37.8	63.3	
			70 Chitosan, 30 Silica (wt%)	78.8	21.2	55.5	
		Chitosan (tested dry)	50 Chitosan, 50 Silica (wt%)	942	271	42.2	
			60 Chitosan, 40 Silica (wt%)	511	161	45.5	
			70 Chitosan, 30 Silica (wt%)	284	141	60.5	
	CH_3COOH (ICPTES)	Chitosan	91 Chitosan (wt%)	1	44.72		[83]
			87 Chitosan (wt%)	2	50.78		
			84 Chitosan (wt%)	4.1	83.04		
			74 Chitosan (wt%)	4.9	96.59		
	HCl	PMMA copolymer (linear structure)	70 PMMA copolymer (wt %)	1.1	75	21	[17]
		PMMA copolymer (random structure)		1	85	23	
		PMMA copolymer (star structure)		0.6	69	28	
	HCl, (ATPES)	TDI	2 TDI (wt%)	36.16	0.67	7.85	[112]
			10 TDI (wt%)	22.15	0.47	16.52	
			20 TDI (wt%)	14.57	0.26	45.93	
	HNO_3 (BTMSH, APTES)	BPGE (epoxy)	30 APTES 20 BTMSH 15 BPGE (mol%)	32.7*	–	2.6 (recovered strain after reaching 25%)*	[113]
			30 APTES 20 BTMSH 18 BPGE (mol%)	35.6*	–	3.4 (recovered strain after reaching 25%)*	
			30 APTES 20 BTMSH 21 BPGE (mol%)	56.1*	–	3.9 (recovered strain after reaching 25%)*	
THEOS	–	CMCD	0.2 CMCD (wt%)	0.00629	0.00128	17.0	[68]
			0.5 CMCD (wt%)	0.01459	0.00236	14.3	
			1 CMCD (wt%)	0.02324	0.00391	14.1	
			1.5 (CMCD (wt%)	0.02388	0.00418	14.1	
			2 CMCD (wt%)	0.02219	0.00366	14.1	
TMOS	–	SA	60 SA, 40 SiO2 (wt%)	0.05	0.21	–	[114]
			40 SA, 60 SiO2 (wt%)	0.48	0.62	–	
			20 SA, 80 SiO2 (wt%)	1.27	1.22	–	
	CH_3CN (APTES)	DI	6.89 DI (wt%)	4.42	187.86	–	[115]
			20.4 DI (wt%)	6.70	216.28	–	
			33.9 DI (wt%)	8.60	186.90	–	
	NH_4OH (APTES)	$C_{15}H_{19}NO_4$ (Tri-Epoxy)	15 Epoxy (vol%)	53.50*	0.778*	–	[116]
			45 Epoxy (vol%)	76.24*	1.121*	–	
			75 Epoxy (vol%)	126.29*	0.888*	–	
	NH_4OH	TMSPM	0.3 TMMA:TMSPM (molar ratio)	0.00173	0.0228	–	[117]
			0.6 TMMA:TMSPM (molar ratio)	0.00093	0.137	–	
			2 TMMA:TMSPM (molar ratio)	0.00333	0.257	–	
	NH_4OH (BTMSH)		20 BTMSH (mol%) 2 TMMA:TMSPM (molar ratio)	0.00677	0.400	–	
			40 BTMSH (mol%) 2 TMMA:TMSPM (molar ratio)	0.00596	0.270	–	
	NH_4OH (BTESB)		5 BTESB (mol%) 2 TMMA:TMSPM (molar ratio)	0.00542	0.131	–	
			10 BTESB (mol%) 2 TMMA:TMSPM (molar ratio)	0.00361	0.279	–	
	NH_4OH (VTMS, BTMSH)	PS		32.43	–	11.10 (unrecovered strain)	[16]

(*continued on next page*)

Table 3 (*continued*)

Silica Precursor	Catalyst (Co-precursor)	Polymer Components	Composition	Avg. Modulus (MPa)	Avg. Ultimate or Maximum Stress (MPa)	Avg. Strain at failure or Maximum Strain (%)	Ref.
			PS 500 FMW with 20 VTMS, 30 BTMSH (mol %)				
			PS 1500 FMW with 20 VTMS,	17.54	–	9.50 (unrecovered strain)	
			30 BTMSH (mol%)	PS 2500 FMW with 20 VTMS, 30 BTMSH (mol %)	18.04	–	
6.70 (unrecovered strain)							
Not reported (polymer modification through SI-ATRP)	–	PMMA	20390 PMMA MW (g mol^{-1})	–	0.0154*	–	[118]
			43013 PMMA MW (g mol^{-1})	–	0.0302*	–	
			63284 PMMA MW (g mol^{-1})	–	0.0485*	–	
			75246 PMMA MW (g mol^{-1})	–	0.0635*	–	

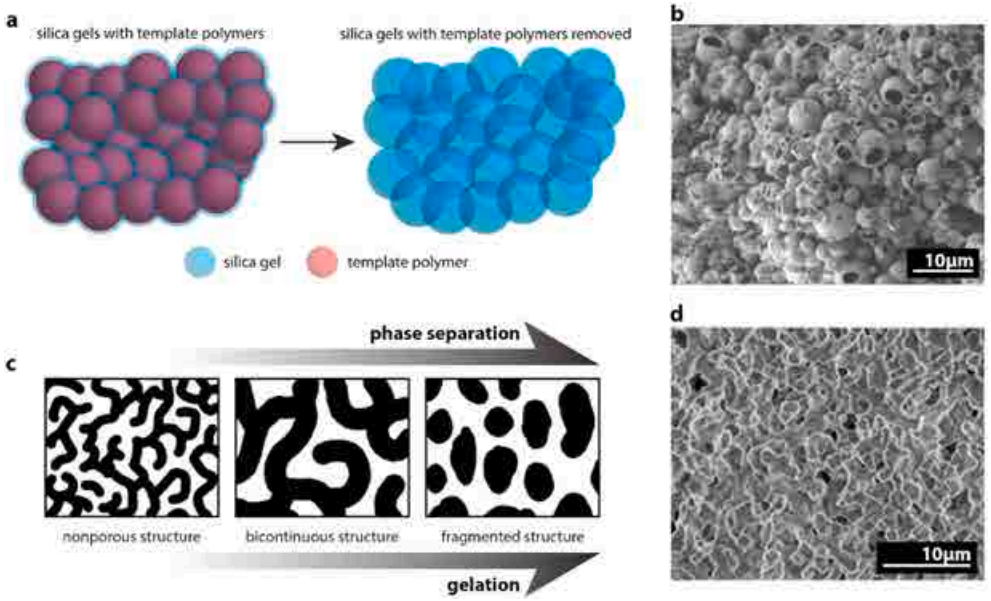

Fig. 7. (a) Illustration of spherical polymer templates used as porogens for high-SSA silica, (b) silica gel after calcination to remove epoxy microspheres taken from Ref. [11], (c) illustration of spinodal decomposition with phase separating polymers taken from Ref. [121], and (d) a co-continuous pore structure achieved with poly (ethylene glycol) as a phase-separating polymer taken from Ref. [49]. Figures were modified from originals and reproduced with permission.

initiate the removal of porogen through dissolution or solvent can be removed later if the aging is required with intact porogen. Advantages of using soluble polymers over hard templating are the ease of forming a co-continuous structure and that the porogen can be removed by a solvent as opposed to more damaging treatments like pyrolysis. Eliminating the need for pyrolysis minimizes the number of processing steps and helps retain the intrinsic surface chemistry and microstructure of the high-SSA silica.

One interesting example of a soluble polymer template is PFA, which controls the pore structure of silica through hydrophobic interactions with TEOS in ethanol [52]. Furfuryl alcohol was added to the silica sol-gel solution with Pluronic F127. Furfuryl alcohol is a hydrophilic organic compound that becomes a hydrophobic polymer during the sol-gel reaction. In solutions with pH range between 2 and 14, silica has anionic surface sites [130–132] and the use of a cationic Pluronic F127 leads to ionic interactions. PFA has also been used with Pluronic F127 [a polyethylene oxide-poly(p-phenylene oxide) block co-polymer also called PEO-PPE] to create hierarchical pores where PFA creates macropores through hydrophobic interactions and Pluronic F127 forms micropores through ionic interactions [52]. Upon the addition of an acid catalyst, furfuryl alcohol polymerizes and becomes hydrophobic, inducing phase separation via nucleation and growth resulting in the formation of macropores. Concurrently, Pluronic F127 acts as a surfactant, forming micelles in the silica-rich phase. Micropores are created as the PEO part of Pluronic F127 reacts to form a shell with a PPE core. Unlike methods that require precise control over the rate of the sol-gel transition and phase separation to obtain hierarchical pores, this method involves the use of a surfactant and a hydrophobic polymer to govern the development of hierarchical pores, thus exhibiting a robust synthesis process.

Surfactants are often used in conjunction with polymeric porogens to reduce the interfacial energy and subsequent agglomeration of immiscible polymers. The surfactant Pluronic F127 [133] discussed above is a class of poloxamer, which are amphiphilic block copolymers [134].

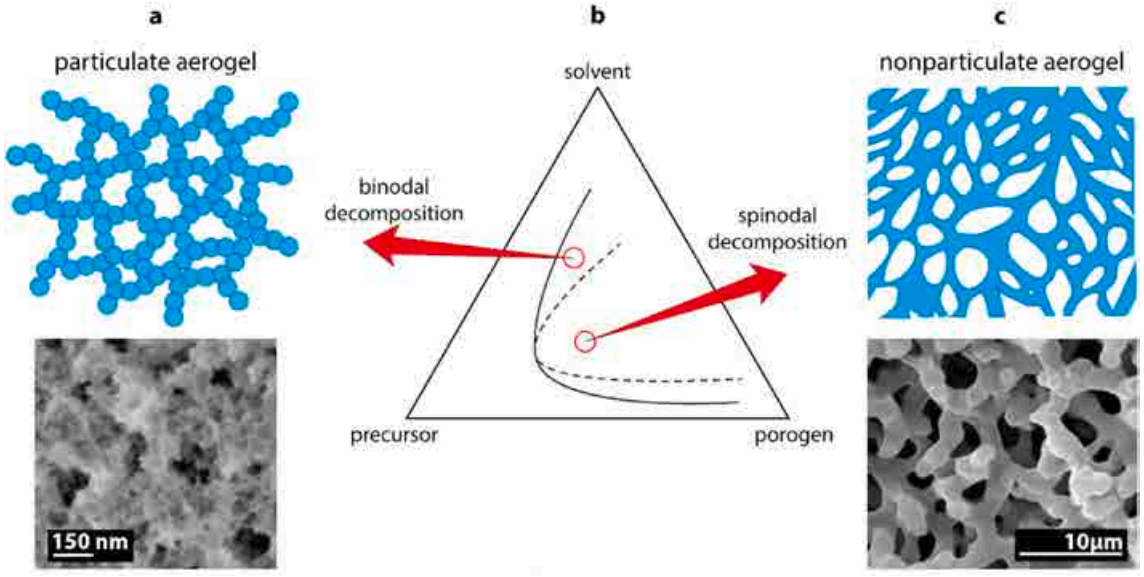

Fig. 8. Pore structure obtained by polymeric phase separation via (a) nucleation and growth (binodal) or (c) spinodal decomposition. This figure was modified from the original and reproduced with permission [7,129].

Pluronic F68 [7] and Pluronic P123 [135,136] are other commercially available poloxamers that act as both porogens and surfactants in the sol-gel process. They are available as liquids, semi-solid pastes, and solids with various chain lengths and numbers of hydrophilic and hydrophobic blocks. In systems using poloxamers as porogens to tailor the microporous structure of the gel, TEOS is often used as a precursor under acidic hydrolysis conditions.

PVA is a water-soluble polymer that has been used with the surfactant sodium dodecyl sulfate (SDS) to create macropores [8]. Although butyl stearate, PVA, and SDS were not removed in this study, they decompose at elevated temperatures, and therefore, pyrolysis could be used to form highly porous silica monoliths [8]. PVA and SDS have also been reacted with the polyester-based precursor (3-glycidyloxypropyl) trimethoxysilane (GPTMS) to form interconnected macropores with silica particles [137]. GPTMS is polymerized using di-tert-butyl peroxide (DTBP) and boron trifluoride diethyl etherate to result in polyethylene and a polyether-based polymeric precursor. The interaction between water and polyether groups in the polymeric precursor induce phase separation. This thermodynamic instability by polymeric precursors can be used to control the particulate and co-continuous structure in silica gels by varying the water to GPTMS ratio. VTMS added as a co-precursor to polymerized GPTMS provided more control over the pore structure [137]. Similar control over thermodynamic instability is possible through the use of other block copolymers, such as poly(ethylene oxide)-block-poly(propylene oxide)-block-poly(ethylene oxide) (i.e., Pluronic P123).

PEG is a hydrophilic polymer extensively studied as porogen in silica gels to create co-continuous pore structures via spinodal decomposition (see Fig. 8). For example, in a study, an aqueous solution of silica sol was prepared with PEG to initiate the sol-gel reaction [122]. In this study, as condensation reactions proceeded, silica-rich and PEG-rich phases are formed. Hydrogen bonding between the PEG and silica led to the distribution of silica in the PEG-rich phase, which produced micropores and mesopores. It was shown that the PEG content in the sol-gel reaction produced macropores, irrespective of the molecular weight of the PEG, while it was observed that PEG with higher molecular weights produces gels with a narrower pore size distributions [122].

PEO, a high-molecular-weight variant of PEG, was used to create interconnected pores in sol-gel reaction [138]. At the beginning of the reaction, droplets of PEO in silica sol grew until they were connected to form an open network [138]. It should be noted that the sol-to-gel transition should be in sync with the phase separation process to obtain the open network structure.

5. Applications

5.1. Energy storage and conversion

As researchers continue to investigate efficient, environment friendly, and cost-effective materials for various applications in the field of energy storage and conversion, polymer-silica composites and hybrids are gaining much attention, especially as solid polymer electrolytes (SPEs) and separators in Li-ion batteries [139,140]. Since conventional liquid electrolytes cannot prevent dendrite formation in Li-ion batteries, researchers have used different polymers to develop safe and efficient SPEs [141,142]. However, SPEs can underperform and decompose over time [143]. As an inorganic filler, silica has been found to improve the performance of SPEs by providing a chemically inert, thermally stable, and interconnected mesoporous substrate that allows for efficient ion transfer across continuous surfaces while inhibiting dendrite formation [144,145].

Amorphous poly(vinyl ethylene carbonate) (PVEC) provides high ionic conductivity as well as high electrochemical stability but, due to its low mechanical strength, it fails to inhibit dendrite formation [35,146]. An SPE based on PVEC-silica composites significantly prevented dendrite formation, while also retaining the intrinsic properties of PVEC [146].

PEO-based SPEs are among the most studied materials in the battery industry because of PEO's high salt-solvating properties [36]. Despite this great potential, the high crystallinity of PEOs suppresses ionic conductivity and limits its commercial applications [147]. Successful efforts to reduce the crystallinity of PEO-based electrolytes have been made through the addition of mesoporous silica fillers [59]. A PEO-based SPE had a reduction in crystallinity from 39.0% to 37.7%, 33.8%, and as low as 23% with the addition of 3 wt%, 10 wt%, and 30 wt % silica, respectively.

Polyetherimide (PEI)-based SPEs have been developed and investigated as PEI is a chemically stable and a mechanically strong polymer with ether (–O–) and isopropylidene ($–C(CH_3)_2–$) groups that can facilitate efficient ion transfer [37]. However, the high water-solubility of PEI limits its energy-related applications. Grafting of PEI with silica led to a considerable reduction in water solubility of PEI making it more

effective for the use in SPEs [58].

Besides silica enhancing common SPEs, some polymers have been observed to enhance the properties of silica in SPEs. A silica-PEG hybrid electrolyte material was developed to improve the ionic conductivity of silica [57]. In this study, the authors investigated the effect of the PEG chain's length (200 and 400 Da) on the resulting hybrid structures. It was observed that, to produce an open hybrid structure that offers higher ionic conductivity, the hybrid should be developed using the shorter PEG chain (200 Da).

To overcome the thermal instability of SPEs, a polymer-silica hybrid was made using trimethylethoxysilane (TMES), GPTMS and ethylene glycol diglycidyl ether (EGDE) epoxy [148]. The hybrid remained stable up to 250 °C, which is higher than the usual Li battery operation range between 20 °C and 60 °C [149]. The hybrid showed improved mechanical properties, electrochemical stability, better Coulombic efficiency, and increased ionic conductivity with increasing EGDE content.

Polymer-modified silica materials were also used for the development of an ionic liquid electrolyte using the sol-gel method with a silica-epoxy scaffold that entrapped an ionic liquid, and was tested for use in Li-ion batteries [150]. The silica-epoxy scaffold provided efficient ion transfer, had a higher ionic conductivity, and required a lower activation energy compared to the ionic liquid electrolyte without silica. The electrolyte remained thermally stable at temperatures up to 195 °C with an impressive electrochemical stability. It also exhibited over 98% Coulombic efficiency.

5.2. Environmental remediation

Sol-gel derived polymer-modified silica has been investigated for environmental remediation due to the availability of high SSAs and surfaces that can be functionalized and tailored to capture specific pollutants [40]. The polymer component is primarily used to provide the mechanical properties needed to withstand operational conditions and enhance the sorption specificities and capacities [38]. Polymer-silica composites have been used in a variety of environmental remediation applications, including heavy metal removal, dye removal, and CO_2 capture.

Heavy metal ion removal using high-SSA silica-polymer composites is a promising approach [53,54]. In one study, polyacrylamide (PAM)-grafted xanthan gum (XG) was used with silica to make a composite adsorbent (PAM-XG-silica) to capture Pb(II) from aqueous media [54]. Adsorption tests based on model Pb(II) solutions showed that a composite containing 0.7 wt% silica exhibited the maximum adsorption capacity of ~220 mg/g after ~125 min. It was observed that this was due to the high hydrodynamic volume. The sorbent showed a Pb(II) removal efficiency of 96.5% when tested against an industrial wastewater. In another study, amine-modified silica was used with PMMA to obtain a composite for the removal of hexavalent chromium Cr(VI) [53]. The composite showed a maximum sorption capacity of 20 mg/g within the pH range of 2–3 at 298 K and reached the equilibrium in 140 min, representing a promising affinity towards Cr(VI) ions.

Silica-polymer composite sorbents have been developed and tested for dye removal from aqueous solutions [55,151]. Inspired by the affinity of PAM-XG-silica composites towards Pb(II) [54], the same group of researchers examined the composite's sorption capacities for Congo Red (CR) dye. As sol-gel derived silica particles were incorporated in PAM-grafted XG copolymer matrix, the SSA of the adsorbent increased from ~26 $m^2\ g^{-1}$ to ~49 $m^2\ g^{-1}$, which facilitated a rapid initial removal rate. The adsorbent exhibited a maximum removal efficiency of 96.37% in 150 min. Effects of pH and temperature on the efficiency of the adsorbent were also examined. The adsorption efficiency of the composite increased from 91.5% to 96.37% when the pH was increased from 2 to 4 and decreased thereafter. The efficiency increased up to 96.37% when a temperature of 318 K was reached and remained unchanged thereafter. Sol-gel-derived silica nanoparticles grafted with quaternary PEI (QPEI) were also used to remove methyl orange from aqueous solutions [55]. The QPEI-silica sorbent showed a sorption capacity 105.4 mg/g within 10 min with only minor changes in the sorption capacity (±0.5 mg/g) over a pH range of 3.2–9.6.

Polymer-silica composites have also been applied in various gas adsorption applications. For example, a mixed-matrix membrane was developed and optimized using a glassy poly(2,6-dimethyl-1,4-phenylene oxide) (PPO)-silica composite to separate H_2 from CO_2 gas [56]. The resulting membrane showed higher H_2 permeation (from 82.2 to 548.7 barrer), which resulted in better H_2/CO_2 separation than native silica. For CO_2 capture, an amine-silica hybrid was developed with varying amounts of APTES as a co-precursor in different ionic liquid environments [152]. Amounts of APTES and ionic liquid showed direct effects on sorption capacity of the hybrid with one variant achieving over 240 mg/g of CO_2 adsorption.

5.3. Scaling and implementation

A recent report estimates the current $300 million global aerogel market should exceed $700 million by 2031 [153]. Silica-based products are the most prevalent type of aerogel primarily due to their superior insulating properties and low density, in addition to the many characteristics discussed previously (see Fig. 9). Despite all the desirable attributes of these high-SSA materials, the high price tag associated with their manufacturing has inhibited their expansion into current markets and new technologies. The main challenge associated with scale-up for manufacturing centers around the question of how to produce large crack-free monoliths in a cost-effective manner [154–156]. Many applications, such thermal insulating blankets and fillers for building material, have bypassed this issue by using granules or powders. However, in some areas, such as ECS and environmental remediation, robust and crack-free monoliths are essential to the success of these technologies. Supercritical drying to produce these monoliths has historically been one of the costliest aspects of the process. However, modeling of the drying processes [157], design of continuous processing, recycling feedstock [158], and optimization of the solvent exchange process [159] are just a few of the methods currently being investigated to reduce the costs limiting scale-up. Advances in ambient pressure drying have also contributed to this goal by reducing the complexity and infrastructure needed to create a gel [159–161]. Efforts are still needed to address issues with microstructural changes during drying, which include compaction and cracking. Tailoring the solvent exchange process to mitigate microstructural changes often leads to the use of more hazardous materials or an increase in the waste volume [162].

Regarding polymer-tailored high-SSA silica, challenges in scaling arise when trying to control the behavior of the polymer during gel synthesis and/or post-synthesis processing. For hybrids and composites, many aspects such as customizing the solvent-polymer compatibility, maintaining passive diffusion capability during gelation, and optimizing the polymer-gel ratio, need to be considered during processing to achieve the desired outcome. For example, as the size of the monolith increases, it becomes harder (and takes longer) to remove the solvent from the inner pores due to diffusion constraints [163]. This issue is compounded when a polymer is present that can further inhibit the fluid migration through the monolith.

Difficulties with solvent removal are exacerbated when polymers are used as porogens because now the polymer must be dissolved and diffuse through the solid during solvent exchanges. Saturation of the solvent with the polymer requires the solvent to be replaced periodically, increasing processing times and waste volumes. Modeling of these processes has been employed to develop an understanding of how the solvent moves through silica aerogels and could be applied to these multi-phase materials to understand how to optimize the exchange process depending on the pore structure and viscosity of the dissolved polymer.

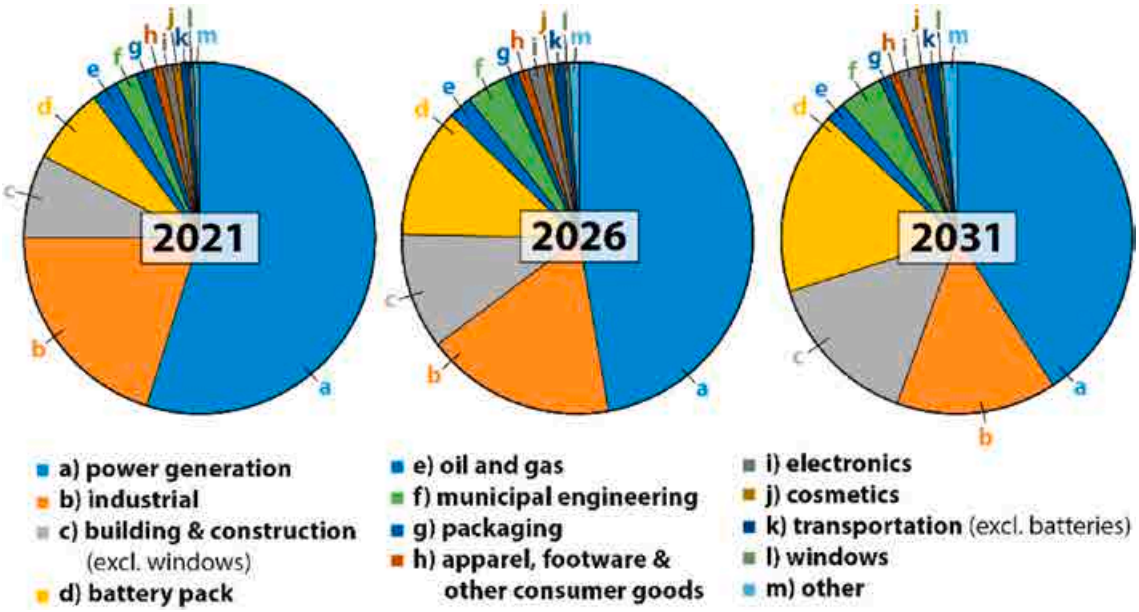

Fig. 9. Revenue of silica aerogel split by application. Figure reproduced with permission [158].

6. Conclusion and future perspectives

The ability to tailor micro/mesoporous silica with polymers is invaluable in enabling this intrinsically brittle material to be utilized in real-world applications. Hybrids and composites combine the beneficial characteristics of silica, such as its ease of formation, functionality, and stability, with the durability of polymers to create tougher materials that can withstand high-temperatures and aqueous environments in which the individual silica materials could not function on their own without sustaining damage. The use of porogens opens a whole new world of applications through the creation of macropores or hierarchical pore structures that allow the materials to be better used as membranes.

There are a few knowledge gaps that, if addressed, can lead to a breakthrough in polymer-tailored silica materials. In particular, the precursor-porogen interactions in the solvent used in sol-gel reactions has not been extensively studied. Understanding the interactions between silica precursors, co-precursors, solvents, catalysts, and polymers is essential to understand the spinodal decomposition, which is critical to increase the intrinsic strength of silica [164]. Suitable drying techniques where the intrinsic properties of the polymer are not affected should be explored to improve the material suitability in various applications [164].

The majority of the processes discussed in this review have only been performed at the bench-scale. Besides the previously discussed solutions to optimize the manufacturing process to assist in scalability, solutions to the cost of the material feedstocks are also needed, as this attributes to almost the same cost as manufacturing in supercritical drying [158]. One solution would be to look towards the use of natural materials or even waste, which would also improve green credentials.

CRediT authorship contribution statement

Karthikeyan Baskaran: Writing – original draft. **Muhammad Ali:** Writing – original draft, Conceptualization. **Katherine Gingrich:** Writing – original draft. **Debora Lyn Porter:** Writing – original draft. **Saehwa Chong:** Writing – original draft. **Brian J. Riley:** Writing – review & editing, Writing – original draft, Conceptualization. **Charles W. Peak:** Writing – review & editing. **Steven E. Naleway:** Writing – review & editing. **Ilya Zharov:** Writing – review & editing. **Krista Carlson:** Writing – review & editing, Writing – original draft, Conceptualization.

Declaration of competing interest

The authors declare that they have no known competing financial interests or personal relationships that could have appeared to influence the work reported in this paper.

Acknowledgements

This work was supported by the United States Department of Energy (DOE) Nuclear Energy University Program (NEUP) under Contract DE-NE0008900. Pacific Northwest National Laboratory (PNNL) is operated by Battelle Memorial Institute for the DOE under contract DE-AC05-76RL01830.

References

[1] K. Lu, Porous and high surface area silicon oxycarbide-based materials—a review, Mater. Sci. Eng. R Rep. 97 (2015) 23–49.
[2] J.L. Gurav, I.-K. Jung, H.-H. Park, E.S. Kang, D.Y. Nadargi, Silica aerogel: synthesis and applications, J. Nanomater. (2010) 1–11, 2010.
[3] T. Woignier, J. Primera, A. Alaoui, P. Etienne, F. Despestis, S. Calas-Etienne, Mechanical properties and brittle behavior of silica aerogels, Gels 1 (2015) 256–275.
[4] C.E. Carraher, General topics: silica aerogels—properties and uses, Polym. News 30 (2005) 386–388.
[5] K.E. Parmenter, F. Milstein, Mechanical properties of silica aerogels, J. Non-Cryst. Solids 223 (1998) 179–189.
[6] K. Baskaran, M. Ali, B.J. Riley, J.S. Bates, I. Zharov, K. Carlson, Membrane synthesis via in-situ pore formation in silica gels through dynamic miscibility with soybean oil, Colloids Surf. A Physicochem. Eng. Asp. 636 (2022) 128183.
[7] J. Chamieh, Y. Zimmermann, A. Boos, A. Hagège, Preparation and characterisation of silica monoliths using a triblock copolymer (F68) as porogen, J. Colloid Interface Sci. 340 (2009) 225–229.
[8] F. Marske, J. Martins De Souza E Silva, R.B. Wehrspohn, T. Hahn, D. Enke, Synthesis of monolithic shape-stabilized phase change materials with high mechanical stability: via a porogen-assisted in situ sol-gel process, RSC Adv. 10 (2020) 3072–3083.
[9] C. Wang, L. Li, S. Zheng, Synthesis and characterization of mesoporous silica monoliths with polystyrene homopolymers as porogens, RSC Adv. 6 (2016) 105840–105853.
[10] W. Xun, Y. Yi, C. Zhang, S. Zheng, Poly(glycidyl methacrylate)-block-poly (ε-caprolactone)- block-poly(glycidyl methacrylate) triblock copolymer: synthesis and use as mesoporous silica porogen, J. Macromol. Sci., Pure Appl. Chem. 50 (2013) 399–410.
[11] X. Yu, C. Zhang, Y. Ni, S. Zheng, Crosslinked epoxy microspheres: preparation, surface-initiated polymerization, and use as macroporous silica porogen, J. Appl. Polym. Sci. 128 (2013) 2829–2839.

[12] F. Akhter, S.A. Soomro, V.J. Inglezakis, Silica aerogels; a review of synthesis, applications and fabrication of hybrid composites, J. Porous Mater. 28 (2021) 1387–1400.
[13] K.-Y. Lee, D.B. Mahadik, V.G. Parale, H.-H. Park, Composites of silica aerogels with organics: a review of synthesis and mechanical properties, J. Kor. Chem. Soc. 57 (2019) 1–23.
[14] C. Li, Y. Huang, X. Feng, Z. Zhang, H. Gao, J. Huang, Silica-assisted cross-linked polymer electrolyte membrane with high electrochemical stability for lithium-ion batteries, J. Colloid Interface Sci. 594 (2021) 1–8.
[15] V.U. Patil, Polymer Reinforced Aerogels and Composites A. Polyimide Crosslinked Aerogels B. Silica-Polymethylmethacrylate Composites, Chemistry, Missouri University Of Science And Technology, 2008.
[16] B.N. Nguyen, M.A.B. Meador, M.E. Tousley, B. Shonkwiler, L. Mccorkle, D. A. Scheiman, A. Palczer, Tailoring elastic properties of silica aerogels cross-linked with polystyrene, ACS Appl. Mater. Interfaces 1 (2009) 621–630.
[17] J.J. Chung, S. Li, M.M. Stevens, T.K. Georgiou, J.R. Jones, Tailoring mechanical properties of sol–gel hybrids for bone regeneration through polymer structure, Chem. Mater. 28 (2016) 6127–6135.
[18] S. Kramer, F. Rubio-Alonso, J.D. Mackenzie, Organically modified silicate aerogels,"aeromosils", MRS Online Proc. 435 (1996) 295–300.
[19] Y. Hu, J.D. Mackenzie, Rubber-like elasticity of organically modified silicates, J. Mater. Sci. 27 (1992) 4415–4420.
[20] G. Philipp, H. Schmidt, New materials for contact lenses prepared from Si-and Ti-alkoxides by the sol-gel process, J. Non-Cryst. Solids 63 (1984) 283–292.
[21] B.J. Deka, E.-J. Lee, J. Guo, J. Kharraz, A.K. An, Electrospun nanofiber membranes incorporating PDMS-aerogel superhydrophobic coating with enhanced flux and improved antiwettability in membrane distillation, Environ. Sci. Technol. 53 (2019) 4948–4958.
[22] E.-J. Lee, B.J. Deka, J. Guo, Y.C. Woo, H.K. Shon, A.K. An, Engineering the re-entrant hierarchy and surface energy of PDMS-PVDF membrane for membrane distillation using a facile and benign microsphere coating, Environ. Sci. Technol. 51 (2017) 10117–10126.
[23] L. Li, B. Yalcin, B.N. Nguyen, M.A.B. Meador, M.J.A.a.m. Cakmak, interfaces, Flexible nanofiber-reinforced aerogel (xerogel) synthesis, manufacture, and characterization, ACS Appl. Mater. Interfaces 1 (2009) 2491–2501.
[24] L. Zhang, G. Feng, X. Li, S. Cui, S. Ying, X. Feng, L. Mi, W. Chen, Synergism of surface group transfer and in-situ growth of silica-aerogel induced high-performance modified polyacrylonitrile separator for lithium/sodium-ion batteries, J. Membr. Sci. 577 (2019) 137–144.
[25] S. Pandey, J. Ramontja, Guar gum-grafted poly (acrylonitrile)-templated silica xerogel: nanoengineered material for lead ion removal, J. Anal. Sci. Technol. 7 (2016) 24.
[26] B.M. Novak, D. Auerbach, C. Verrier, Low-density, mutually interpenetrating organic-inorganic composite materials via supercritical drying techniques, Chem. Mater. 6 (1994) 282–286.
[27] B.L. Abramoff, L.C. Klein, PMMA-impregnated Silica Gels: Synthesis and Characterization, Sol-Gel Optics, International Society for Optics and Photonics, 1990, pp. 241–248.
[28] K. Khezri, H. Mahdavi, Polystyrene-silica aerogel nanocomposites by in situ simultaneous reverse and normal initiation technique for ATRP, Microporous Mesoporous Mater. 228 (2016) 132–140.
[29] K. Yang, M. Venkataraman, J. Karpiskova, Y. Suzuki, S. Ullah, I.-S. Kim, J. Militky, Y. Wang, T. Yang, J. Wiener, Structural analysis of embedding polyethylene glycol in silica aerogel, Microporous Mesoporous Mater. 310 (2021) 110636.
[30] C. Zhao, Y. Yan, Z. Hu, L. Li, X. Fan, Preparation and characterization of granular silica aerogel/polyisocyanurate rigid foam composites, Construct. Build. Mater. 93 (2015) 309–316.
[31] K. Kanamori, M. Aizawa, K. Nakanishi, T.J.J.o.s.-g.s. Hanada, technology, Elastic organic–inorganic hybrid aerogels and xerogels, J. Sol. Gel Sci. Technol. 48 (2008) 172–181.
[32] O. Pinchuk, F. Dundar, A. Ata, K. Wynne, Improved thermal stability, properties, and electrocatalytic activity of sol-gel silica modified carbon supported Pt catalysts, Int. J. Hydrogen Energy 37 (2012) 2111–2120.
[33] A. Guyomard-Lack, J. Abusleme, P. Soudan, B. Lestriez, D. Guyomard, J. L. Bideau, Hybrid silica-polymer ionogel solid electrolyte with tunable properties, Adv. Energy Mater. 4 (2014) 1301570.
[34] A. Feinle, N. Hüsing, Mixed metal oxide aerogels from tailor-made precursors, J. Supercrit. Fluids 106 (2015) 2–8.
[35] Z. Lin, X. Guo, Z. Wang, B. Wang, S. He, L.A. O'Dell, J. Huang, H. Li, H. Yu, L. Chen, A wide-temperature superior ionic conductive polymer electrolyte for lithium metal battery, Nano Energy 73 (2020) 104786.
[36] X. Yang, M. Jiang, X. Gao, D. Bao, Q. Sun, N. Holmes, H. Duan, S. Mukherjee, K. Adair, C. Zhao, J. Liang, W. Li, J. Li, Y. Liu, H. Huang, L. Zhang, S. Lu, Q. Lu, R. Li, C.V. Singh, X. Sun, Determining the limiting factor of the electrochemical stability window for PEO-based solid polymer electrolytes: main chain or terminal –OH group? Energy Environ. Sci. 13 (2020) 1318–1325.
[37] G. Wang, Y. Weng, D. Chu, D. Xie, R. Chen, Preparation of alkaline anion exchange membranes based on functional poly(ether-imide) polymers for potential fuel cell applications, J. Membr. Sci. 326 (2009) 4–8.
[38] H. Maleki, L. Duraes, A. Portugal, An overview on silica aerogels synthesis and different mechanical reinforcing strategies, J. Non-Cryst. Solids 385 (2014) 55–74.
[39] K. Lee, D. Mahadik, V. Parale, H. Park, Composites of silica aerogels with organics: a review of synthesis and mechanical properties, J. Kor. Chem. Soc. 57 (2020) 1–23.
[40] G. Kaya, H. Deveci, Synergistic effects of silica aerogels/xerogels on properties of polymer composites: a review, J. Ind. Eng. Chem. 89 (2020) 13–27.
[41] T. Linhares, M.P.d. Amorim, L. Durães, Silica aerogel composites with embedded fibres: a review on their preparation, properties and applications, J. Mater. Chem. 7 (2019) 22768–22802.
[42] S. Alwin, X. Shajan, Aerogels: promising nanostructured materials for energy conversion and storage applications, Mater. Renew. Sustain. Energy 9 (2020).
[43] S. Karamikamkar, H.E. Naguib, C.B. Park, Advances in precursor system for silica-based aerogel production toward improved mechanical properties, customized morphology, and multifunctionality: a review, Adv. Colloid Interface Sci. 276 (2020) 102101.
[44] S. Salimian, A. Zadhoush, Z. Talebi, B. Fischer, P. Winiger, F. Winnefeld, S. Zhao, M. Barbezat, M. Koebel, W. Malfait, Silica aerogel-epoxy nanocomposites: understanding epoxy reinforcement in terms of aerogel surface chemistry and epoxy-silica interface compatibility, ACS Appl. Nano Mater. 1 (2018) 4179–4189.
[45] S. Zhao, Z. Zhang, G. Sèbe, R. Wu, R.V. Rivera Virtudazo, P. Tingaut, M. M. Koebel, Multiscale Assembly of superinsulating silica aerogels within silylated nanocellulosic scaffolds: improved mechanical properties promoted by nanoscale chemical compatibilization, Adv. Funct. Mater. 25 (2015) 2326–2334.
[46] Z. Li, L. Gong, X. Cheng, S. He, C. Li, H. Zhang, Flexible silica aerogel composites strengthened with aramid fibers and their thermal behavior, Mater. Des. 99 (2016) 349–355.
[47] M. Shi, C. Tang, X. Yang, J. Zhou, F. Jia, Y. Han, Z. Li, Superhydrophobic silica aerogels reinforced with polyacrylonitrile fibers for adsorbing oil from water and oil mixtures, RSC Adv. 7 (2017) 4039–4045.
[48] H. Lee, D. Lee, J. Cho, Y.-O. Kim, S. Lim, S. Youn, Y.C. Jung, S.Y. Kim, D.G. Seong, Super-insulating, flame-retardant, and flexible poly(dimethylsiloxane) composites based on silica aerogel, Compos. Appl. Sci. Manuf. 123 (2019) 108–113.
[49] W. Wang, T. Li, H. Long, L. Zhu, Preparation of hierarchically mesoporous silica monolith using two components of poly(ethylene glycol) as cooperative dual-templates, J. Non-Cryst. Solids 461 (2017) 80–86.
[50] D. Kuang, T. Brezesinski, B. Smarsly, Hierarchical porous silica materials with a trimodal pore system using surfactant templates, J. Am. Chem. Soc. 126 (2004) 10534–10535.
[51] F. Li, Z. Wang, N.S. Ergang, C.A. Fyfe, A. Stein, Controlling the shape and alignment of mesopores by confinement in colloidal crystals: designer pathways to silica monoliths with hierarchical porosity, Langmuir 23 (2007) 3996–4004.
[52] G.L. Drisko, A. Zelcer, R.A. Caruso, G.J.D.A.A. Soler-Illia, One-pot synthesis of silica monoliths with hierarchically porous structure, Microporous Mesoporous Mater. 148 (2012) 137–144.
[53] M. Dinari, R. Soltani, G. Mohammadnezhad, Kinetics and thermodynamic study on novel modified–mesoporous silica MCM-41/polymer matrix nanocomposites: effective adsorbents for trace CrVI removal, J. Chem. Eng. Data 62 (2017) 2316–2329.
[54] S. Ghorai, A. Sinhamahpatra, A. Sarkar, A.B. Panda, S. Pal, Novel biodegradable nanocomposite based on XG-g-PAM/SiO2: application of an efficient adsorbent for Pb2+ ions from aqueous solution, Bioresour. Technol. 119 (2012) 181–190.
[55] J. Liu, S. Ma, L. Zang, Preparation and characterization of ammonium-functionalized silica nanoparticle as a new adsorbent to remove methyl orange from aqueous solution, Appl. Surf. Sci. 265 (2013) 393–398.
[56] G.-L. Zhuang, H.-H. Tseng, M.-Y. Wey, Preparation of PPO-silica mixed matrix membranes by in-situ sol–gel method for H2/CO2 separation, Int. J. Hydrogen Energy 39 (2014) 17178–17190.
[57] J.F. Vélez, M. Aparicio, J. Mosa, Effect of lithium salt in nanostructured silica–polyethylene glycol solid electrolytes for Li-ion battery applications, J. Phys. Chem. C 120 (2016) 22852–22864.
[58] Y. Wang, J. Ren, M. Deng, Ultrathin solid polymer electrolyte PEI/Pebax2533/AgBF4 composite membrane for propylene/propane separation, Separ. Purif. Technol. 77 (2011) 46–52.
[59] J. Xi, X. Qiu, X. Ma, M. Cui, J. Yang, X. Tang, W. Zhu, L. Chen, Composite polymer electrolyte doped with mesoporous silica SBA-15 for lithium polymer battery, Solid State Ionics 176 (2005) 1249–1260.
[60] C. Brinker, G. Scherer, Sol-Gel Science: the Physics and Chemistry of Sol-Gel Processing, Academic Press, Inc, 1990.
[61] A. Pierre, Introduction to Sol-Gel Processing Springer, 2020.
[62] O.A. Shilova, Synthesis and structure features of composite silicate and hybrid TEOS-derived thin films doped by inorganic and organic additives, J. Sol. Gel Sci. Technol. 68 (2013) 387–410.
[63] H. Yu, X. Liang, J. Wang, M. Wang, S. Yang, Preparation and characterization of hydrophobic silica aerogel sphere products by co-precursor method, Solid State Sci. 48 (2015) 155–162.
[64] M. Aegerter, N. Leventis, Aerogels Handbook, Springer, 2011.
[65] Aerogel Handbook, Springer, 2011.
[66] B. Wang, A. Reifsnyder, I. Zharov, K. Carlson, Silica aerogel membranes fabricated using removable nitrocellulose scaffolds, Microporous Mesoporous Mater. 278 (2019) 435–442.
[67] H. Choi, V.G. Parale, T. Kim, Y.-S. Choi, J. Tae, H.-H. Park, Structural and mechanical properties of hybrid silica aerogel formed using triethoxy(1-phenylethenyl)silane, Microporous Mesoporous Mater. (2020) 298.
[68] Z. Cai, J. Wu, M. Wu, R. Li, P. Wang, H. Zhang, Rheological characterization of novel carboxymethylated curdlan-silica hybrid hydrogels with tunable mechanical properties, Carbohydr. Polym. 230 (2020) 115578.
[69] M. Megahed, D.E. Tobbala, M.A.A. El-baky, The effect of incorporation of hybrid silica and cobalt ferrite nanofillers on the mechanical characteristics of glass fiber-reinforced polymeric composites, Polym. Compos. 42 (2020) 271–284.

[70] L. Chen, S. Chai, K. Liu, N. Ning, J. Gao, Q. Liu, F. Chen, Q. Fu, Enhanced epoxy/silica composites mechanical properties by introducing graphene oxide to the interface, ACS Appl. Mater. Interfaces 4 (2012) 4398–4404.
[71] J. Zhu, J. Hu, C. Jiang, S. Liu, Y. Li, Ultralight, hydrophobic, monolithic konjac glucomannan-silica composite aerogel with thermal insulation and mechanical properties, Carbohydr. Polym. 207 (2019) 246–255.
[72] R. Eslami, R. Bagheri, Y. Hashemzadeh, M. Salehi, Optical and mechanical properties of transparent acrylic based polyurethane nano Silica composite coatings, Prog. Org. Coating 77 (2014) 1184–1190.
[73] D.K. Rajak, D.D. Pagar, R. Kumar, C.I. Pruncu, Recent progress of reinforcement materials: a comprehensive overview of composite materials, J. Mater. Res. Technol. 8 (2019) 6354–6374.
[74] Z.Y. Liu, S.J. Xu, B.L. Xiao, P. Xue, W.G. Wang, Z.Y. Ma, Effect of ball-milling time on mechanical properties of carbon nanotubes reinforced aluminum matrix composites, Compos. Appl. Sci. Manuf. 43 (2012) 2161–2168.
[75] E. Pullicino, W. Zou, M. Gresil, C. Soutis, The effect of shear mixing speed and time on the mechanical properties of GNP/epoxy composites, Appl. Compos. Mater. 24 (2016) 301–311.
[76] C. Sanchez, K.J. Shea, S. Kitagawa, Recent progress in hybrid materials science, Chem. Soc. Rev. 40 (2011) 471–472.
[77] P. Judeinstein, C. Sanchez, Hybrid organic–inorganic materials: a land of multidisciplinarity, J. Mater. Chem. 6 (1996) 511–525.
[78] C. Sanchez, G.J.D.A.A. Soler-Illia, F. Ribot, D. Grosso, Design of functional nano-structured materials through the use of controlled hybrid organic–inorganic interfaces, Compt. Rendus Chem. 6 (2003) 1131–1151.
[79] G. Kickelbick, Hybrid Materials: Synthesis, Characterization, and Applications, John Wiley & Sons, 2007.
[80] Z. Fei, Z. Yang, G. Chen, K. Li, Preparation of tetraethoxysilane-based silica aerogels with polyimide cross-linking from 3, 3′, 4, 4′-biphenyltetracarboxylic dianhydride and 4, 4′-oxydianiline, J. Sol. Gel Sci. Technol. 85 (2018) 506–513.
[81] T. Zhou, X. Cheng, Y. Pan, C. Li, L. Gong, H. Zhang, Mechanical performance and thermal stability of glass fiber reinforced silica aerogel composites based on co-precursor method by freeze drying, Appl. Surf. Sci. 437 (2018) 321–328.
[82] Y. Zhao, Y. Li, R. Zhang, Silica aerogels having high flexibility and hydrophobicity prepared by sol-gel method, Ceram. Int. 44 (2018) 21262–21268.
[83] A. Pipattanawarothai, C. Suksai, K. Srisook, T. Trakulsujaritchok, Non-cytotoxic hybrid bioscaffolds of chitosan-silica: sol-gel synthesis, characterization and proposed application, Carbohydr. Polym. 178 (2017) 190–199.
[84] P. Maximiano, L. Durães, P. Simões, Intermolecular interactions in composites of organically-modified silica aerogels and polymers: a molecular simulation study, Microporous Mesoporous Mater. 314 (2021) 110838.
[85] J. Chen, J. Liu, Y. Yao, S. Chen, Effect of Microstructural Damage on the Mechanical Properties of Silica Nanoparticle-Reinforced Silicone Rubber Composites, Engineering Fracture Mechanics, 2020, p. 235.
[86] D.W. Lee, B.R. Yoo, Advanced silica/polymer composites: materials and applications, J. Ind. Eng. Chem. 38 (2016) 1–12.
[87] H. Sai, L. Xing, J. Xiang, L. Cui, J. Jiao, C. Zhao, Z. Li, F. Li, T. Zhang, Flexible aerogels with interpenetrating network structure of bacterial cellulose–silica composite from sodium silicate precursor via freeze drying process, RSC Adv. 4 (2014) 30453.
[88] J. Jaxel, G. Markevicius, A. Rigacci, T. Budtova, Thermal superinsulating silica aerogels reinforced with short man-made cellulose fibers, Compos. Appl. Sci. Manuf. 103 (2017) 113–121.
[89] F. Jiang, S. Hu, Y.-L. Hsieh, Aqueous synthesis of compressible and thermally stable cellulose nanofibril–silica aerogel for CO2 adsorption, ACS Appl. Nano Mater. 1 (2018) 6701–6710.
[90] R. Ciriminna, A. Fidalgo, V. Pandarus, F. Béland, L. Ilharco, M. Pagliaro, The sol-gel route to advanced silica-based materials and recent applications, Chem. Rev. 113 (2013) 6592–6620.
[91] A. Fidalgo, J.P.S. Farinha, J.M.G. Martinho, M.E. Rosa, L.M. Ilharco, Hybrid silica/polymer aerogels dried at ambient pressure, Chem. Mater. 19 (2007) 2603–2609.
[92] J. Fu, S. Wang, C. He, Z. Lu, J. Huang, Z. Chen, Facilitated fabrication of high strength silica aerogels using cellulose nanofibrils as scaffold, Carbohydr. Polym. 147 (2016) 89–96.
[93] M. Cai, S. Shafi, Y. Zhao, Preparation of compressible silica aerogel reinforced by bacterial cellulose using tetraethylorthosilicate and methyltrimethoxylsilane co-precursor, J. Non-Cryst. Solids 481 (2018) 622–626.
[94] L.M. Ilharco, A. Fidalgo, J.P.S. Farinha, J.M.G. Martinho, M.E.L. Rosa, Nanostructured silica/polymer subcritical aerogels, J. Mater. Chem. 17 (2007) 2195.
[95] R. Arat, H. Baskan, G. Ozcan, P. Altay, Hydrophobic silica-aerogel integrated polyacrylonitrile nanofibers, J. Ind. Textil. (2020), https://doi.org/10.1177/1528083720939670.
[96] S.K. Nataraj, K.S. Yang, T.M. Aminabhavi, Polyacrylonitrile-based nanofibers—a state-of-the-art review, Prog. Polym. Sci. 37 (2012) 487–513.
[97] T. Nazir, A. Afzal, H.M. Siddiqi, Z. Ahmad, M. Dumon, Thermally and mechanically superior hybrid epoxy–silica polymer films via sol–gel method, Prog. Org. Coating 69 (2010) 100–106.
[98] A.I. Romero, M.L. Parentis, A.C. Habert, E.E. Gonzo, Synthesis of polyetherimide/silica hybrid membranes by the sol–gel process: influence of the reaction conditions on the membrane properties, J. Mater. Sci. 46 (2011) 4701–4709.
[99] K. Ebisike, A.E. Okoronkwo, K.K. Alaneme, Synthesis and characterization of Chitosan–silica hybrid aerogel using sol-gel method, J. King Saud Univ. Sci. 32 (2020) 550–554.
[100] M.R. Rejab, M.H. Hamdan, M. Quanjin, J.P. Siregar, D. Bachtiar, Y. Muchlis, Historical development of hybrid materials, Mat. Sci. Mat. Eng 4 (2020) 445–455.
[101] J.D. Mackenzie, Structures and properties of ormosils, J. Sol. Gel Sci. Technol. 2 (1994) 81–86.
[102] J.D. Mackenzie, E.P. Bescher, Structures, properties and potential applications of ormosils, J. Sol. Gel Sci. Technol. 13 (1998) 371–377.
[103] L. Zhong, X. Chen, H. Song, K. Guo, Z. Hu, Highly flexible silica aerogels derived from methyltriethoxysilane and polydimethylsiloxane, New J. Chem. 39 (2015) 7832–7838.
[104] S. Zhao, Y. Yan, A. Gao, S. Zhao, J. Cui, G. Zhang, Flexible polydimethylsilane nanocomposites enhanced with a three-dimensional graphene/carbon nanotube bicontinuous framework for high-performance electromagnetic interference shielding, ACS Appl. Mater. Interfaces 10 (2018) 26723–26732.
[105] Y. Tang, Q. Zheng, B. Chen, Z. Ma, S. Gong, A new class of flexible nanogenerators consisting of porous aerogel films driven by mechanoradicals, Nano Energy 38 (2017) 401–411.
[106] Y.-Z. Lin, L.-B. Zhong, S. Dou, Z.-D. Shao, Q. Liu, Y.-M. Zheng, Facile synthesis of electrospun carbon nanofiber/graphene oxide composite aerogels for high efficiency oils absorption, Environ. Int. 128 (2019) 37–45.
[107] A. Dourani, M. Haghgoo, M. Hamadanian, Multi-walled carbon nanotube and carbon nanofiber/polyacrylonitrile aerogel scaffolds for enhanced epoxy resins, Composites, Part B 176 (2019) 107299.
[108] Y. Wu, Y. Xie, F. Zhong, J. Gao, J. Yao, Fabrication of bimetallic Hofmann-type metal-organic Frameworks@ Cellulose aerogels for efficient iodine capture, Microporous Mesoporous Mater. 306 (2020) 110386.
[109] Y. Liao, Z. Pang, X. Pan, Fabrication and mechanistic study of aerogels directly from whole biomass, ACS Sustain. Chem. Eng. 7 (2019) 17723–17736.
[110] X. Zhang, H. Wang, Z. Cai, N. Yan, M. Liu, Y. Yu, Highly compressible and hydrophobic anisotropic aerogels for selective oil/organic solvent absorption, ACS Sustain. Chem. Eng. 7 (2019) 332–340.
[111] J.N. Liang, L.P. Yan, Y.F. Dong, X. Liu, G. Wu, N.R. Zhao, Robust and nanostructured chitosan-silica hybrids for bone repair application, J. Mater. Chem. B 8 (2020) 5042–5051.
[112] H. Yang, X. Kong, Y. Zhang, C. Wu, E. Cao, Mechanical properties of polymer-modified silica aerogels dried under ambient pressure, J. Non-Cryst. Solids 357 (2011) 3447–3453.
[113] M.A.B. Meador, C.M. Scherzer, S.L. Vivod, D. Quade, B.N. Nguyen, Epoxy reinforced aerogels made using a streamlined process, ACS Appl. Mater. Interfaces 2 (2010) 2162–2168.
[114] J.-S. Oh, J.-S. Park, C.-M. Han, E.-J. Lee, Facile in situ formation of hybrid gels for direct-forming tissue engineering, Mater. Sci. Eng. C 78 (2017) 796–805.
[115] M.A.B. Meador, L.A. Capadona, L. Mccorkle, D.S. Papadopoulos, N. Leventis, Structure−Property relationships in porous 3D nanostructures as a function of preparation conditions: isocyanate cross-linked silica aerogels, Chem. Mater. 19 (2007) 2247–2260.
[116] M.A.B. Meador, E.F. Fabrizio, F. Ilhan, A. Dass, G. Zhang, P. Vassilaras, J. C. Johnston, N. Leventis, Cross-linking amine-modified silica aerogels with epoxies: mechanically strong lightweight porous materials, Chem. Mater. 17 (2005) 1085–1098.
[117] H. Maleki, L. Durães, A. Portugal, Synthesis of lightweight polymer-reinforced silica aerogels with improved mechanical and thermal insulation properties for space applications, Microporous Mesoporous Mater. 197 (2014) 116–129.
[118] D.J. Boday, P.Y. Keng, B. Muriithi, J. Pyun, D.A. Loy, Mechanically reinforced silica aerogel nanocomposites via surface initiated atom transfer radical polymerizations, J. Mater. Chem. 20 (2010) 6863.
[119] M. Iwata, T. Adachi, M. Tomidokoro, M. Ohta, T. Kobayashi, Hybrid sol–gel membranes of polyacrylonitrile–tetraethoxysilane composites for gas permselectivity, J. Appl. Polym. Sci. 88 (2003) 1752–1759.
[120] N. Hüsing, U. Schubert, Aerogels—airy materials: chemistry, structure, and properties, Angew. Chem. Int. Ed. 37 (1998) 22–45.
[121] J. Konishi, K. Fujita, K. Nakanishi, K. Hirao, Monolithic TiO2with controlled multiscale porosity via a template-free Sol−Gel process accompanied by phase separation, Chem. Mater. 18 (2006) 6069–6074.
[122] T. Hara, G. Desmet, G.V. Baron, H. Minakuchi, S. Eeltink, Effect of polyethylene glycol on pore structure and separation efficiency of silica-based monolithic capillary columns, J. Chromatogr. A 1442 (2016) 42–52.
[123] K. Nakanishi, N. Soga, Phase separation in silica sol–gel system containing poly (ethylene oxide) II. Effects of molecular weight and temperature, Bull. Chem. Soc. Jpn. 70 (1997) 587–592.
[124] R. Cademartiri, M.A. Brook, R. Pelton, J.D. Brennan, Macroporous silica using a "sticky" Stöber process, J. Mater. Chem. 19 (2009) 1583–1592.
[125] K. Nakanishi, Porous gels made by phase separation: recent progress and future directions, J. Sol. Gel Sci. Technol. 19 (2000) 65–70.
[126] K. Nakanishi, R. Takahashi, T. Nagakane, K. Kitayama, N. Koheiya, H. Shikata, N. Soga, Formation of hierarchical pore structure in silica gel, J. Sol. Gel Sci. Technol. 17 (2000) 191–210.
[127] K. Nakanishi, N. Soga, Phase separation in gelling silica–organic polymer solution: systems containing poly(sodium styrenesulfonate), J. Am. Ceram. Soc. 74 (1991) 2518–2530.
[128] K. Nakanishi, N. Tanaka, Sol-gel with phase separation. Hierarchically porous materials optimized for high-performance liquid chromatography separations, Acc. Chem. Res. 40 (2007) 863–873.
[129] X. Chen, B. Put, A. Sagara, K. Gandrud, M. Murata, J.A. Steele, H. Yabe, T. Hantschel, M. Roeffaers, M. Tomiyama, H. Arase, Y. Kaneko, M. Shimada, M. Mees, P.M. Vereecken, Silica gel solid nanocomposite electrolytes with

interfacial conductivity promotion exceeding the bulk Li-ion conductivity of the ionic liquid electrolyte filler, Sci. Adv. 6 (2020), eaav3400.
[130] N.N. Greenwood, A. Earnshaw, Chemistry of the Elements, Elsevier Science, 2012.
[131] K. Ikari, K. Suzuki, H. Imai, Structural control of mesoporous silica nanoparticles in a binary surfactant system, Langmuir 22 (2006) 802–806.
[132] M. Eftekhari, K. Schwarzenberger, A. Javadi, K. Eckert, The influence of negatively charged silica nanoparticles on the surface properties of anionic surfactants: electrostatic repulsion or the effect of ionic strength? Phys. Chem. Chem. Phys. 22 (2020) 2238–2248.
[133] K. Kanamori, Y. Kodera, G. Hayase, K. Nakanishi, T. Hanada, Transition from transparent aerogels to hierarchically porous monoliths in polymethylsilsesquioxane sol-gel system, J. Colloid Interface Sci. 357 (2011) 336–344.
[134] I. Schmolka, Polyoxyethylene-polyoxypropylene Aqueous Gels, Google Patents, 1973.
[135] S. Tao, Y. Wang, Y. An, Superwetting monolithic SiO2 with hierarchical structure for oil removal, J. Mater. Chem. 21 (2011) 11901–11907.
[136] S. Flaig, J. Akbarzadeh, H. Peterlik, N. Hüsing, Hierarchically organized silica monoliths: influence of different acids on macro- and mesoporous formation, J. Sol. Gel Sci. Technol. 73 (2015) 103–111.
[137] S. Rezaei, A.M. Zolali, A. Jalali, C.B. Park, Novel and simple design of nanostructured, super-insulative and flexible hybrid silica aerogel with a new macromolecular polyether-based precursor, J. Colloid Interface Sci. 561 (2020) 890–901.
[138] O.Y. Vodorezova, I.N. Lapin, T.I. Izaak, Formation of the open-cell foam structures in tetraethoxysilane-based gelling systems, J. Sol. Gel Sci. Technol. 94 (2020) 384–392.
[139] K.S. Ngai, S. Ramesh, K. Ramesh, J.C. Juan, A review of polymer electrolytes: fundamental, approaches and applications, Ionics 22 (2016) 1259–1279.
[140] M. Yanilmaz, Y. Lu, J. Zhu, X. Zhang, Silica/polyacrylonitrile hybrid nanofiber membrane separators via sol-gel and electrospinning techniques for lithium-ion batteries, J. Power Sources 313 (2016) 205–212.
[141] D. Koo, S. Ha, D.-M. Kim, K.T. Lee, Recent approaches to improving lithium metal electrodes, Curr. Opin. Electrochem. 6 (2017) 70–76.
[142] B. Commarieu, A. Paolella, J.-C. Daigle, K. Zaghib, Toward high lithium conduction in solid polymer and polymer–ceramic batteries, Curr. Opin. Electrochem. 9 (2018) 56–63.
[143] S. Kaboli, H. Demers, A. Paolella, A. Darwiche, M. Dontigny, D. Clément, A. Guerfi, M.L. Trudeau, J.B. Goodenough, K. Zaghib, Behavior of solid electrolyte in Li-polymer battery with NMC cathode via in-situ scanning electron microscopy, Nano Lett. 20 (2020) 1607–1613.
[144] D. Lin, P.Y. Yuen, Y. Liu, W. Liu, N. Liu, R.H. Dauskardt, Y. Cui, A silica-aerogel-reinforced composite polymer electrolyte with high ionic conductivity and high modulus, Adv. Mater. 30 (2018) 1802661.
[145] S. Liu, N. Imanishi, T. Zhang, A. Hirano, Y. Takeda, O. Yamamoto, J. Yang, Effect of nano-silica filler in polymer electrolyte on Li dendrite formation in Li/poly (ethylene oxide)–Li(CF3SO2)2N/Li, J. Power Sources 195 (2010) 6847–6853.
[146] Y. Kuai, F. Wang, J. Yang, H. Lu, Z. Xu, X. Xu, Y. Nuli, J. Wang, Silica-nanoresin crosslinked composite polymer electrolyte for ambient-temperature all-solid-state lithium batteries, Mater. Chem. Front. 5 (2021) 6502–6511.
[147] L. Xu, J. Li, W. Deng, L. Li, G. Zou, H. Hou, L. Huang, X. Ji, Boosting the ionic conductivity of PEO electrolytes by waste eggshell-derived fillers for high-performance solid lithium/sodium batteries, Mater. Chem. Front. 5 (2021) 1315–1323.
[148] J.F. Vélez, M. Aparicio, J. Mosa, Covalent silica-PEO-LiTFSI hybrid solid electrolytes via sol-gel for Li-ion battery applications, Electrochim. Acta 213 (2016) 831–841.
[149] S. Ma, M. Jiang, P. Tao, C. Song, J. Wu, J. Wang, T. Deng, W. Shang, Temperature effect and thermal impact in lithium-ion batteries: a review, Prog. Nat. Sci.: Mater. Int. 28 (2018) 653–666.
[150] F. Wu, N. Chen, R. Chen, L. Wang, L. Li, Organically modified silica-supported ionogels electrolyte for high temperature lithium-ion batteries, Nano Energy 31 (2017) 9–18.
[151] S. Ghorai, A.K. Sarkar, A.B. Panda, S. Pal, Effective removal of Congo red dye from aqueous solution using modified xanthan gum/silica hybrid nanocomposite as adsorbent, Bioresour. Technol. 144 (2013) 485–491.
[152] M. Garip, N. Gizli, Ionic liquid containing amine-based silica aerogels for CO2 capture by fixed bed adsorption, J. Mol. Liq. 310 (2020) 113227.
[153] R. Collins, Aerogels 2021-2031: Technologies, Markets and Players, IDTechEx Ltd, 2021.
[154] I. Smirnova, P. Gurikov, Aerogel production: current status, research directions, and future opportunities, J. Supercrit. Fluids 134 (2018) 228–233.
[155] M. Rubin, C.M. Lampert, Transparent silica aerogels for window insulation, Sol. Energy Mater. 7 (1983) 393–400.
[156] K.I. Jensen, J.M. Schultz, Highly Insulating and Light Transmitting Aerogel Glazing for Window (HILIT Aerogel Window): Publishable Final Report, 2001.
[157] A.E. Lebedev, A.M. Katalevich, N.V. Menshutina, Modeling and scale-up of supercritical fluid processes. Part I: supercritical drying, J. Supercrit. Fluids 106 (2015) 122–132.
[158] R. Collins, Why Isn't the Aerogel Industry Booming?, IDTechEx, 2019.
[159] M. Schwan, S. Nefzger, B. Zoghi, C. Oligschleger, B. Milow, Improvement of solvent exchange for supercritical dried aerogels, Front. Mater. 8 (2021).
[160] J. Wang, Y. Wei, W. He, X. Zhang, A versatile ambient pressure drying approach to synthesize silica-based composite aerogels, RSC Adv. 4 (2014) 51146–51155.
[161] M.M. Koebel, L. Huber, S. Zhao, W.J. Malfait, Breakthroughs in cost-effective, scalable production of superinsulating, ambient-dried silica aerogel and silica-biopolymer hybrid aerogels: from laboratory to pilot scale, J. Sol. Gel Sci. Technol. 79 (2016) 308–318.
[162] M. Tobiszewski, J. Namieśnik, F. Pena-Pereira, Environmental risk-based ranking of solvents using the combination of a multimedia model and multi-criteria decision analysis, Green Chem. 19 (2017) 1034–1042.
[163] B.J. Riley, S. Chong, R.M. Asmussen, A. Bourchy, M.H. Engelhard, Polyacrylonitrile composites of Ag–Al–Si–O aerogels and xerogels as iodine and iodide sorbents, ACS Appl. Polym. Mater. 3 (2021) 3344–3353.
[164] S. Rezaei, A. Jalali, A.M. Zolali, M. Alshrah, S. Karamikamkar, C.B. Park, Robust, ultra-insulative and transparent polyethylene-based hybrid silica aerogel with a novel non-particulate structure, J. Colloid Interface Sci. 548 (2019) 206–216.